Final Report on Project No. 20ST.23440-4-9168

CONTRACT REPORT NO. OST84-00268

IDENTIFICATION OF RESIDUAL PHASES IN LEACHED MIDWEST LAKE URANIUM ORE

by

W. Charles Cooper and Roy O. Ifill
Department of Metallurgical Engineering
Queen's University
Kingston, Ontario
K7L 3N6

Prepared for Energy, Mines and Resources Canada

March 1985

93 pp

OCT 30 1985
MICROMEDIA

ABSTRACT

Ground samples of unleached and leached Midwest Lake uranium ore were subjected to mineral identification by optical techniques and semi-quantitative, electron microprobe analysis.

Autoradiography has revealed low-intensity radioactivity to be uniformly distributed throughout the ore and residues of the HCl, H_2SO_4, HNO_3 and Cl_2 leaches. Scanning electron microscopy has established the absence of surface coatings from the ore and residue particles. Hence, the uniform, low-intensity radioactivity has been interpreted as manifestations of adsorbed radioactive species, identification of which was not possible. It is considered that the HCl-O_2 pressure-leach and $FeCl_3$ leach systems effectively prevented such adsorption. The autoradiographs have also identified $FeCl_3$ and H_2SO_4 as the most effective lixiviants for dissolving the ore minerals, pitchblende and coffinite.

1. INTRODUCTION

Various uranium leaching processes have been investigated in the search for one which can consistently produce tailings containing environmentally acceptable concentrations of ^{228}Ra. Whereas, a leaching process might be effective in dissolving approximately 100% of the uranium from the ore, significantly less than 100% of the radium is retained in solution. This observation has, therefore, indicated the need for determining the behaviour of radium during leaching and its chemical mode of residence in the tailings.

The current project was initiated to determine whether any precipitates, possibly as discrete grains or coatings on gangue particles, resulted from leaching, and whether ^{226}Ra resides in such precipitates.

2. EXPERIMENTAL PROCEDURE

One ground sample of unleached Midwest Lake uranium ore and six of leach residues were supplied by CANMET. A small portion of each sample, as received, was mixed with a cold-setting resin to a viscous consistency, which just permitted flow, and mounted in a 30-mm diameter plastic ring in which the mixture hardened overnight. The sample surfaces were ground on 220-grit silicon carbide particles in water on a rotating wheel, and then successively refined on 400- and 1000-grit particles in water on glass plates. Polishing was accomplished by a Dürener automatic polisher in which 6-μm, 3-μm and 1-μm diamond pastes in oil were used in turn. The polished mounts were labelled as follows:

unleached ore: MWL-1 and -1A (2 mounts)

$FeCl_3$ leach residue: MWL-2

HCl leach residue: MWL-3

HCl-O_2 pressure-leach residue: MWL-4

H_2SO_4 leach residue: MWL-5

HNO_3 leach residue: MWL-6

Cl_2 leach residue: MWL-7.

Mineral identification was initiated with the unleached ore by polarized-light microscopy, and the observed range of minerals was recorded in photomicrographs. Optical examination of the leach-residue samples then followed and a careful search was conducted for surface coatings and discrete precipitates, the ore samples being used for comparison.

Autoradiographs, which served to map the distribution of radionuclides in the unleached ore and leach-residue samples, were pre-

pared by exposing Kodak NS-2T No-screen X-ray film to the polished sample surfaces for 74 hours. Afterwards, the film and samples together were exposed briefly to white light to outline the autoradiographs. The film was then developed and prints were made in a manner which facilitated direct comparison with the samples.

Mineral identification was confirmed by semi-quantitative analysis on the electron microprobe from which X-ray spectra were generated at 20 keV.

A scanning electron microscope was employed to reveal surface details which are beyond the resolving power of the optical microscope.

3. ORE MINERALOGY

3.1 Ore Minerals

The ore minerals in Midwest Lake ore are pitchblende and coffinite. Pitchblende occurs as two grey, intergrown phases (Figure 1): the lighter-grey phase is connoted by Dahlkamp (1978) as "pitchblende I" or "pseudopitchblende", and is deficient in uranium (U_3O_7) relative to UO_2; the darker-grey phase is termed "pitchblende II" or "sooty pitchblende" (op. cit.), and incorporates a superabundance of oxygen (U_3O_{8+x}) relative to U_3O_7. Pitchblende is commonly intergrown with galena (Figures 2a, 2b and 2c) and, in the absence of galena, contains unsulphidized Pb (Figure 2b) which appears to be residual from the assimilation of galena. Berman (1957) has identified massicotite (orthorhombic PbO) as the form of unsulphidized Pb in uraninite.

Coffinite is of slightly lower reflectance than sooty pitchblende (Figures 3a and 3b), and is commonly intergrown with gersdorffite (NiAsS) (Figure 3c). The X-ray spectrum for coffinite (Figure 3b) reveals the almost invariable presence of minor proportions of Ni, As and S.

3.2 Gangue Minerals

Of these minerals, gersdorffite is the most abundant, accounting for about 60% of the gangue mineral occurrences. It occurs as individual

Figure 1

(a) Pitchblende grain: light-grey phase is pitchblende I and dark-grey phase is sooty pitchblende. Numerous white inclusions are inferred to be galena.

(b) X-ray spectrum of pitchblende I (analysed at point 1 in grain).

(c) X-ray spectrum of pitchblende II (analysed at point 3).

PITCHBLENDE 1

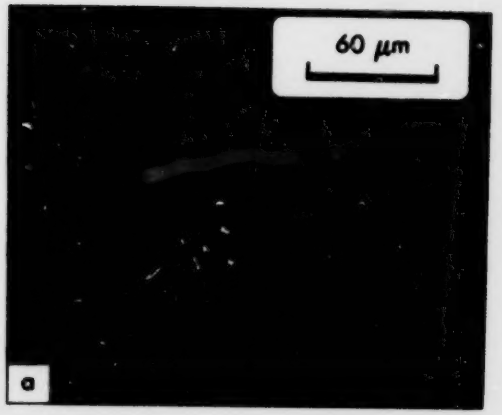

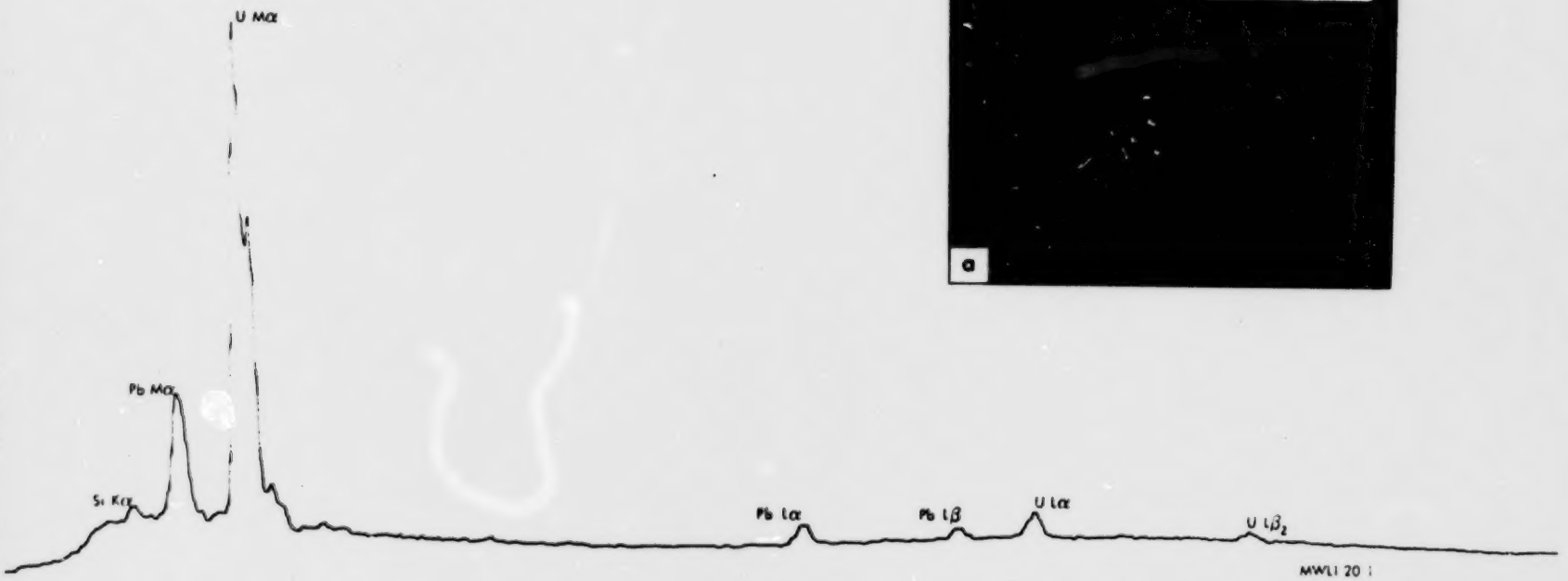

v. f. s. 32k

(vertical full scale = 32 000 intensity units)

b

PITCHBLENDE II

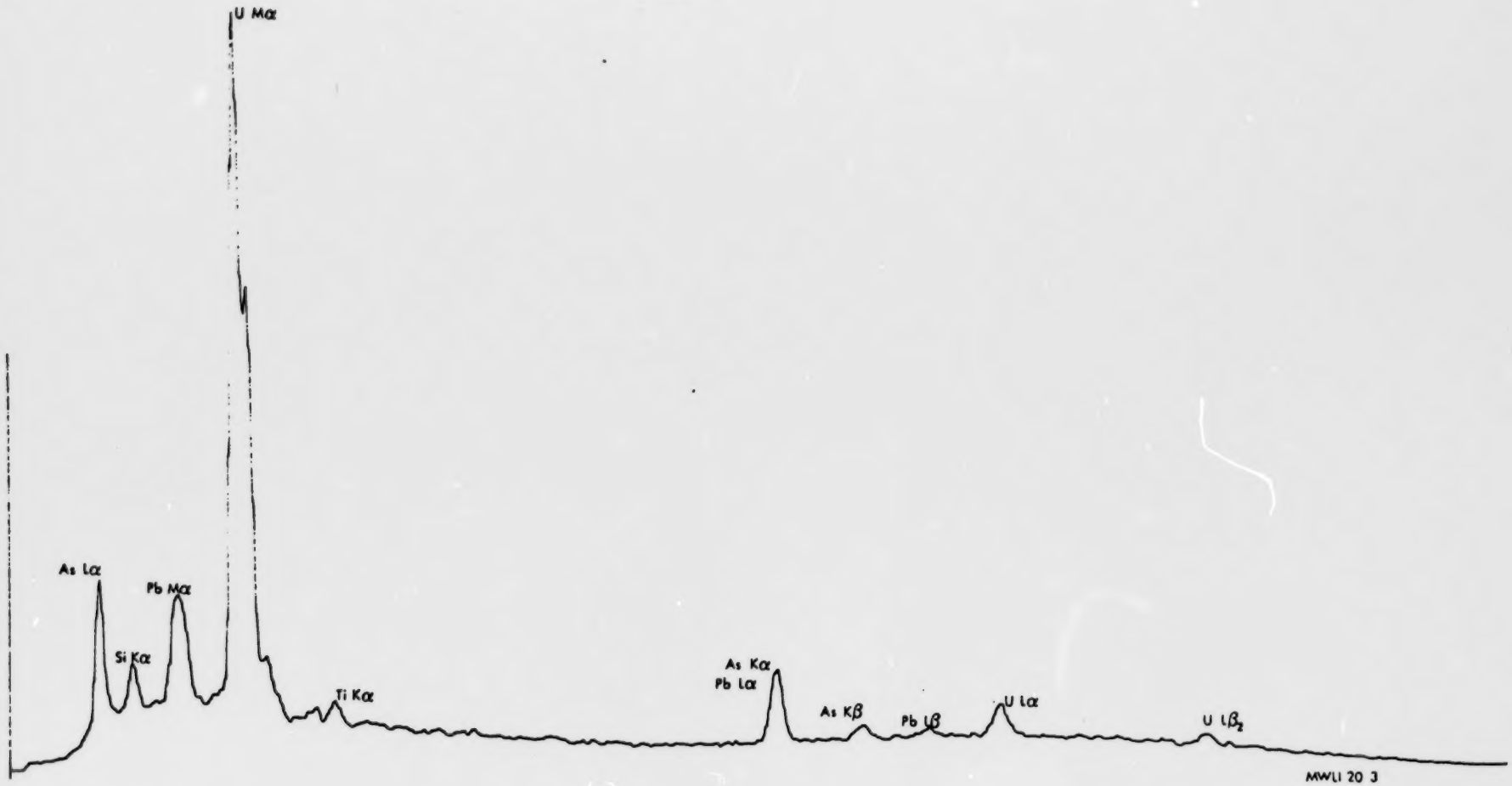

v. f. s. 16k

C

Figure 2

(a) Pitchblende grain incorporating coffinite intergrowths. Lightest-grey phase is pitchblende I, darker-grey is sooty pitchblende, and dark-grey phase at extreme right of grain is coffinite.

(b) X-ray spectrum of pitchblende I (analysed at point 2).

(c) X-ray spectrum of galena (point 6).

(d) X-ray spectrum of point 4 in grain.

PITCHBLENDE 1

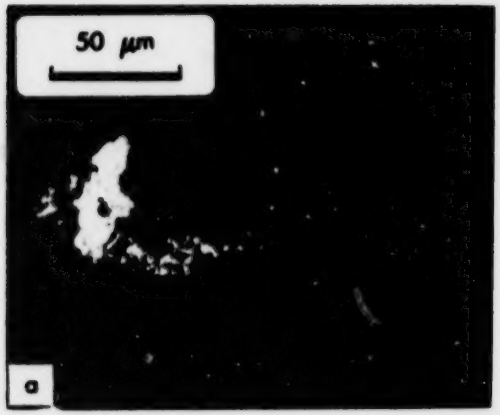

b

GALENA

v. f. s. 65k

C

PITCHBLENDE–COFFINITE intergrowth with minor GERSDORFFITE

v. f. s. 16k

d

Figure 3

(a) White grain is gersdorffite. it is also included in the smaller, dark-grey grain which is coffinite.

(b) X-ray spectrum of coffinite.

(c) X-ray spectrum of gersdorffite inclusion in coffinite.

(d) X-ray spectrum of gersdorffite grain.

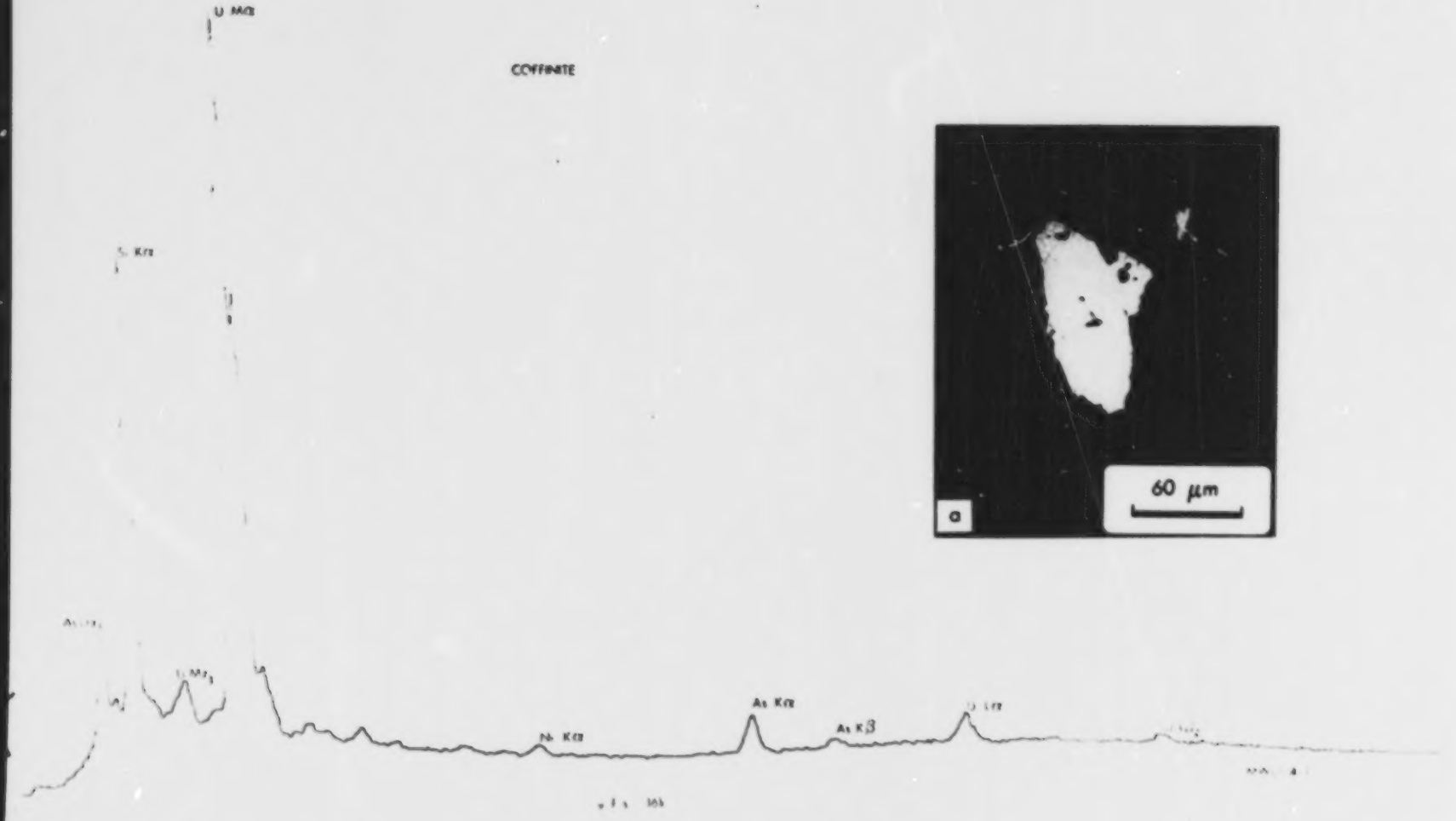
U Mα
COFFINITE
Si Kα
60 μm
a
As Kα
As Kβ
Ni Kα
b

GERSDORFFITE

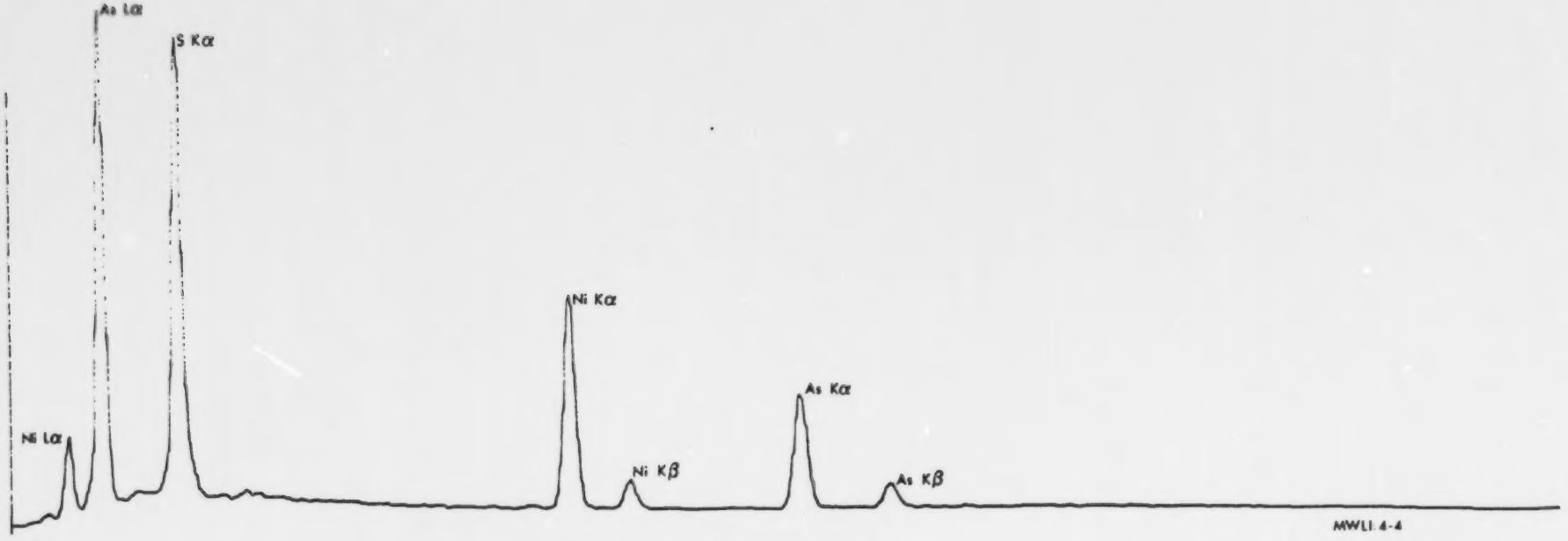

v. f. s. 32k

C

GERSDORFFITE

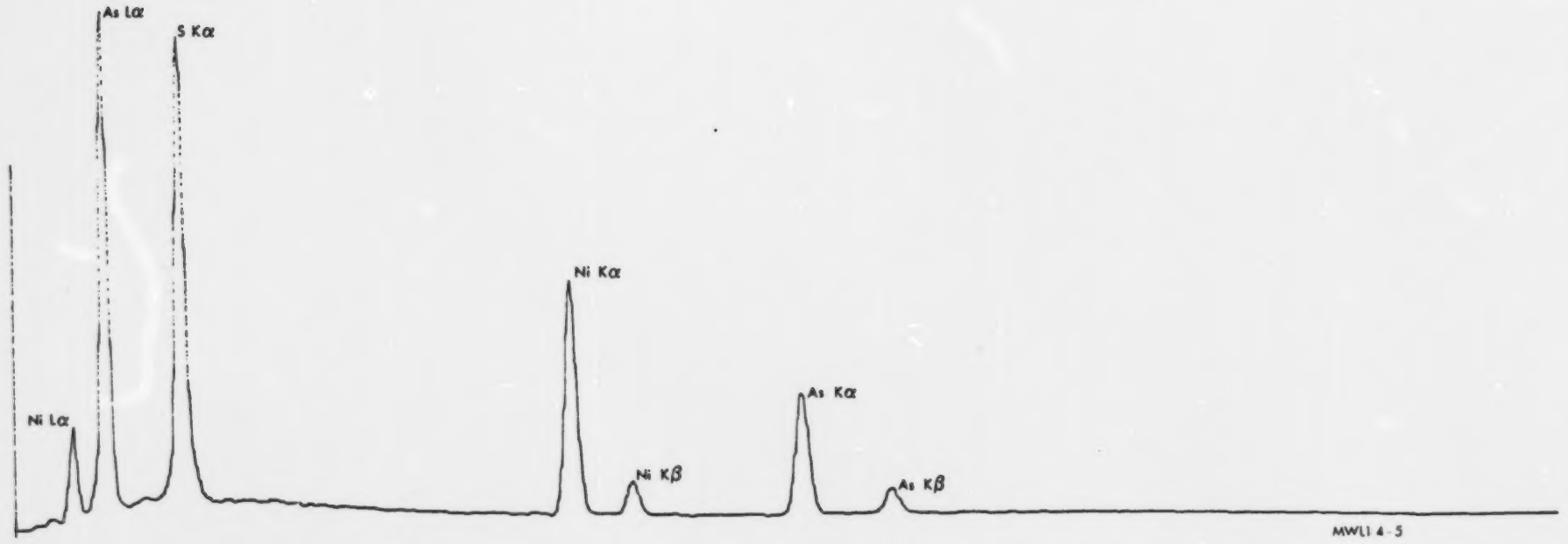

v. f. s. 32k

d

grains (Figures 3a and 3d), and as inclusions in coffinite (Figures 3a and 3b).

Individual grains of galena have not been observed; the mineral appears to exist mainly as inclusions in pitchblende (Figures 2a and 2c).

In Midwest Lake ore, unlike in Elliot Lake ore, the major iron-bearing minerals are magnetite, hematite and goethite which, together, constitute about 30-35% of the gangue mineral occurrences. They are evident as individual grains (Figures 4a, 4b, 5a and 5b)and as composite bands (Figures 6a to 6d). S and As are often present in minor tenors.

Pyrite occurrences have been observed to be limited to inclusion in gersdorffite (Figures 7a to 7c) and sphalerite (Figures 8a to 8c), the latter host-mineral itself not occurring in any significant abundance.

Zircon occurs as semi-transparent grains in the silicate matrix, and commonly exhibits chemical zonation due to enrichment in yttrium (Figures 9a to 9c) or other elements (Figures 10a to 10c).

Titania (probably rutile or anatase) has been observed as transparent grains (Figures 11a and 11b).

Chalcopyrite was sparsely distributed as tiny fragments in the samples. No occurrences of millerite (NiS), niccolite (NiAs), bravoite ($[Fe,Ni]S_2$) or rammelsbergite ($NiAs_2$) were observed.

Figure 4

(a) Goethite single grain.

(b) X-ray spectrum of goethite.

GOETHITE

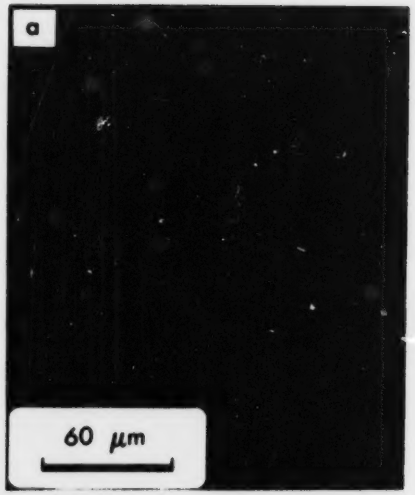

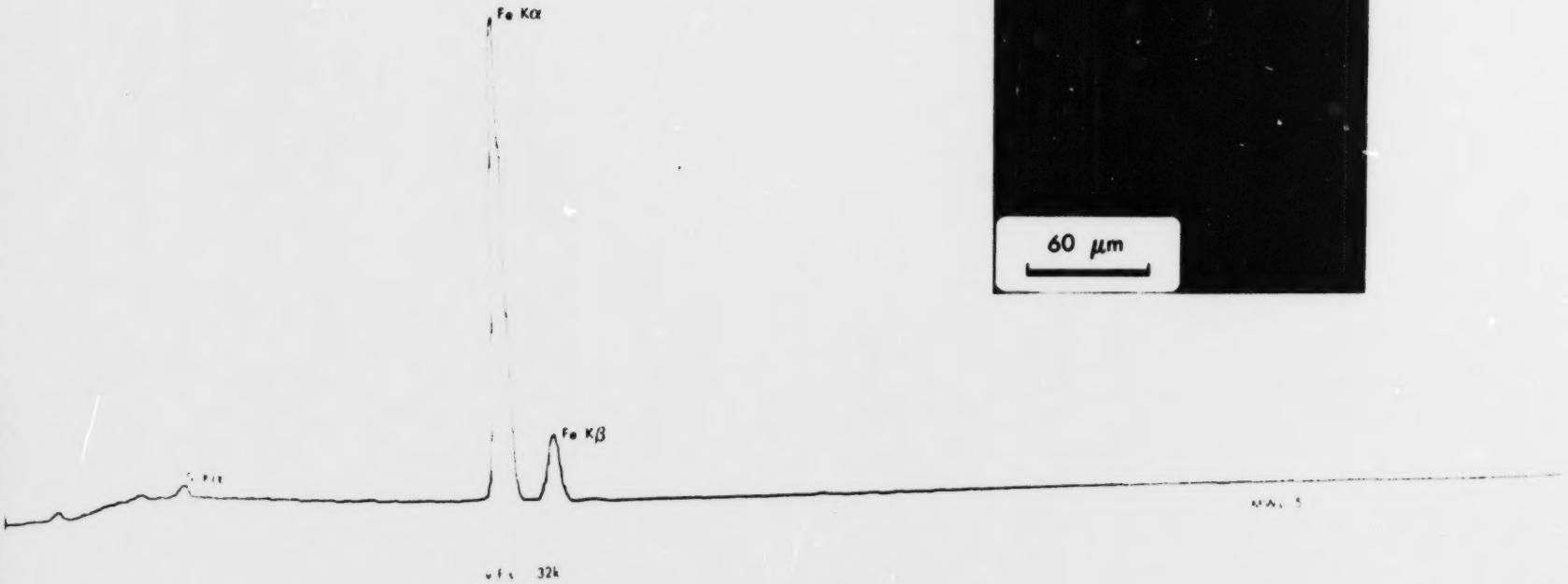

b

Figure 5

(a) Hematite single grain. The lighter-grey patches are residue from the carbon coat applied to the sample prior to electron microprobe analysis.

(b) X-ray spectrum of hematite.

HEMATITE

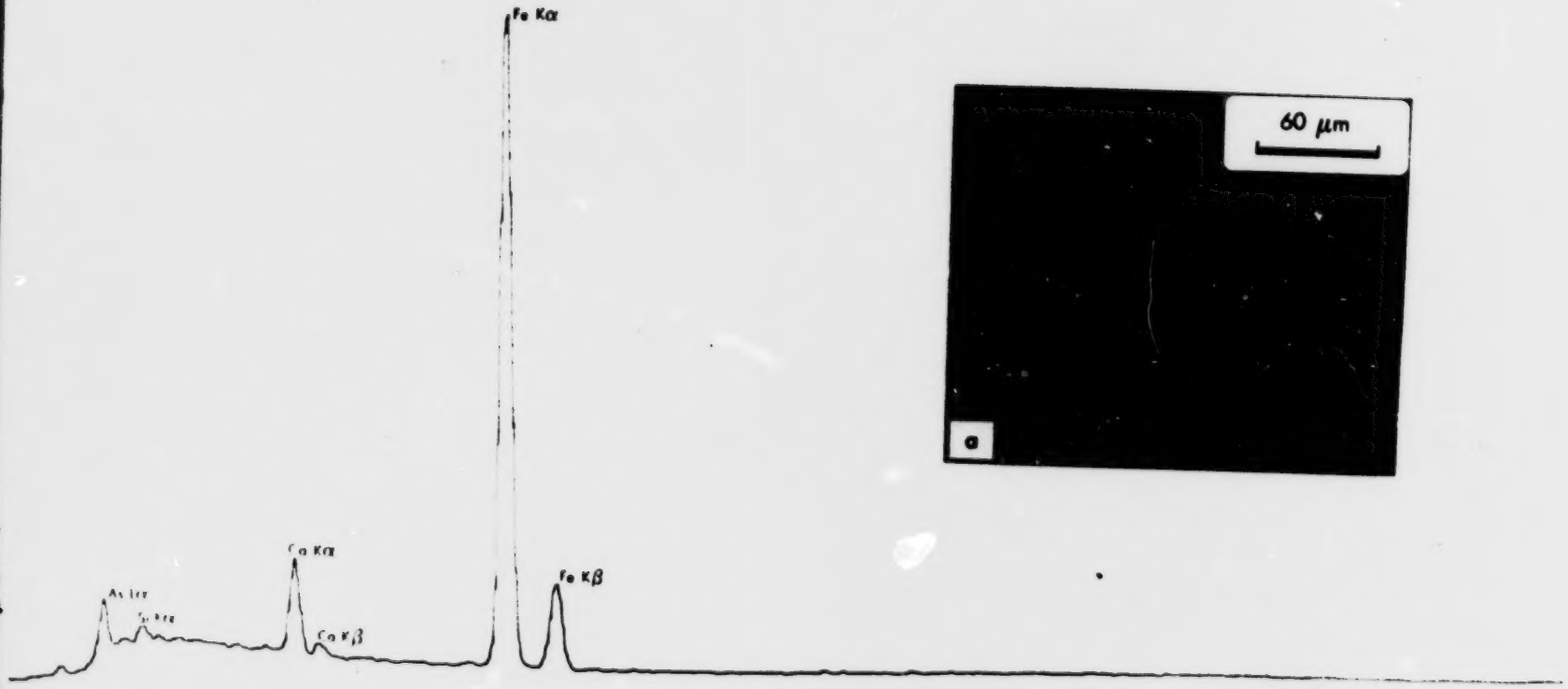

b

Figure 6

(a) Composite grain: lightest-grey band is magnetite, darker-grey bands are goethite, and darkest-grey band at the bottom of the grain is hematite. Small white, adjacent grain is gersdorffite.

(b) X-ray spectrum of goethite.

(c) X-ray spectrum of magnetite.

(d) X-ray spectrum of hematite.

GOETHITE

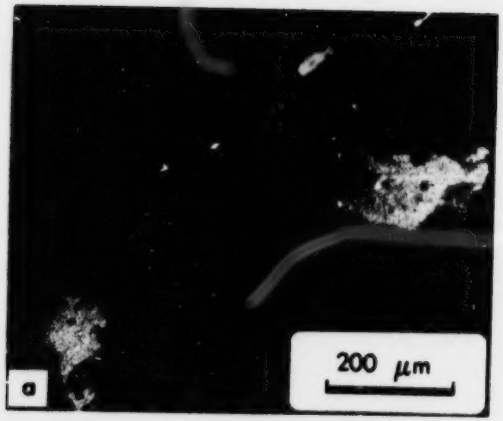

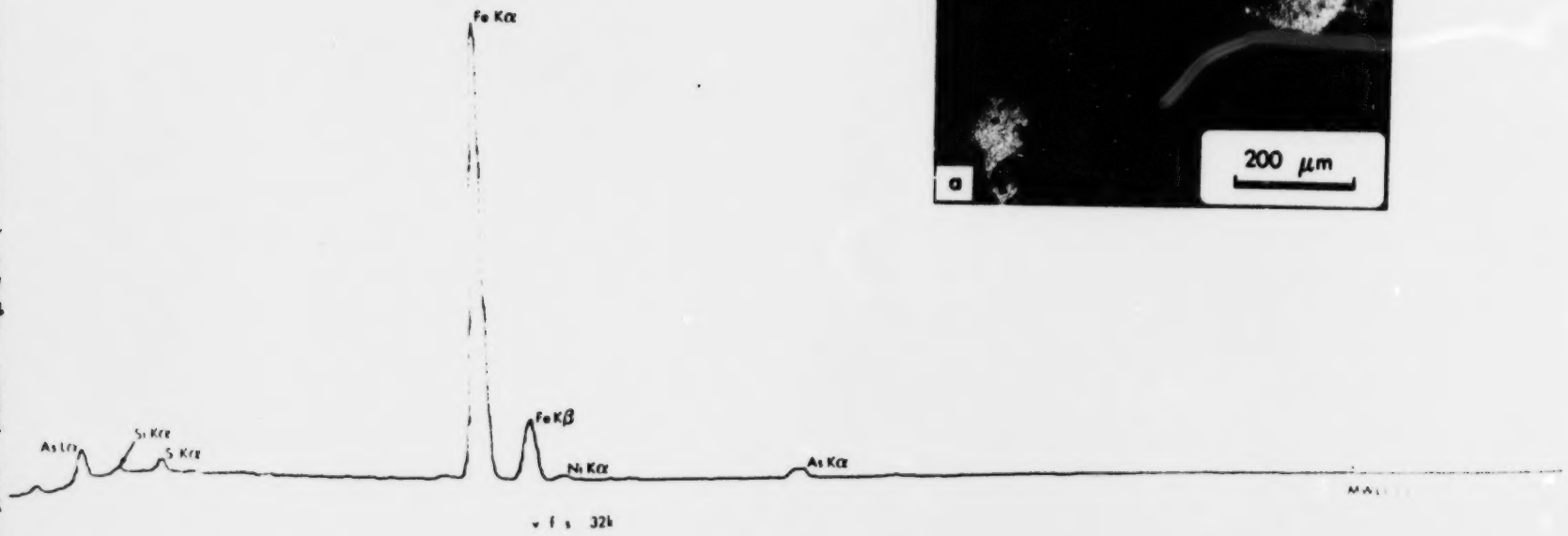

b

MAGNETITE

v. f. s. 32k

C

HEMATITE with minor GERSDORFFITE

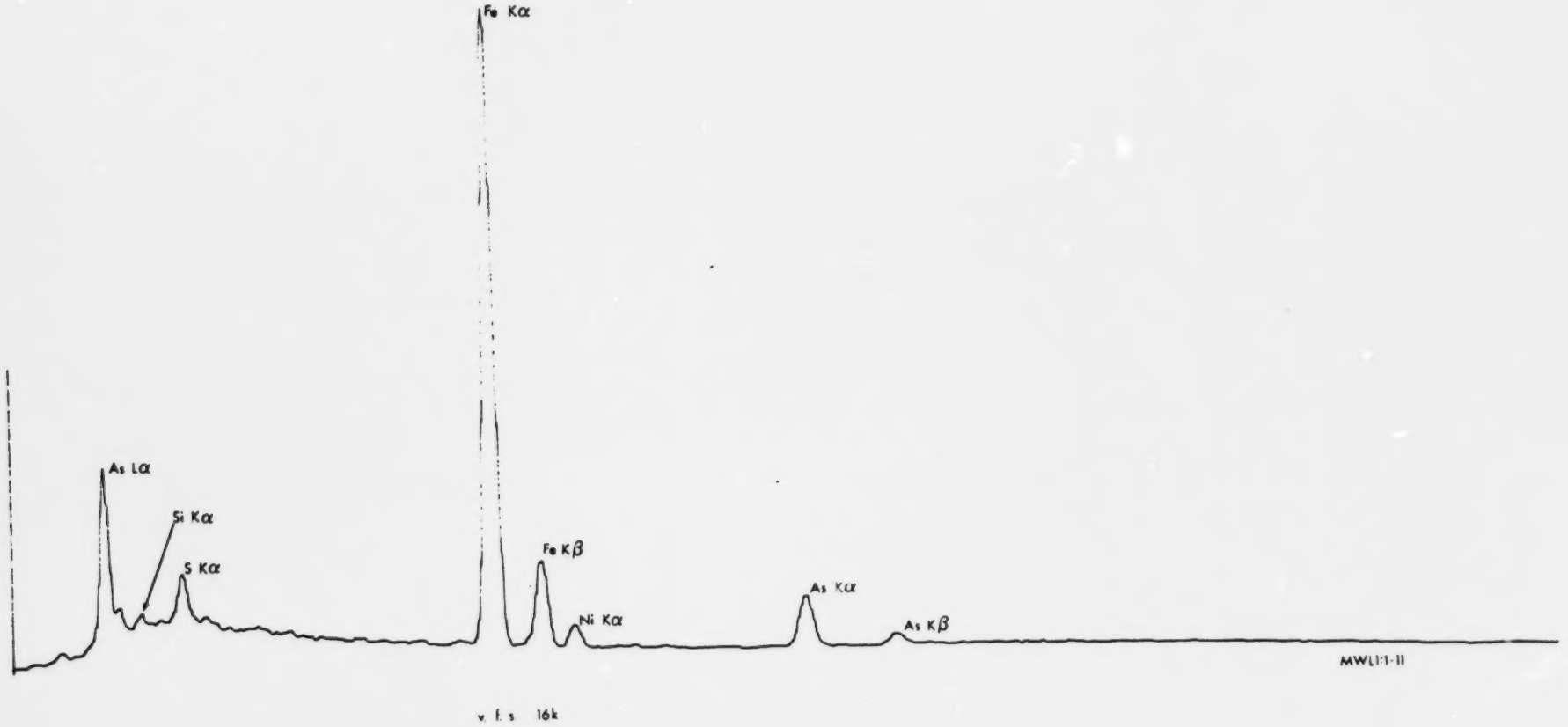

d

Figure 7

(a) Gersdorffite surrounding a pyrite grain.

(b) X-ray spectrum of gersdorffite.

(c) X-ray spectrum of pyrite.

GERSDORFFITE

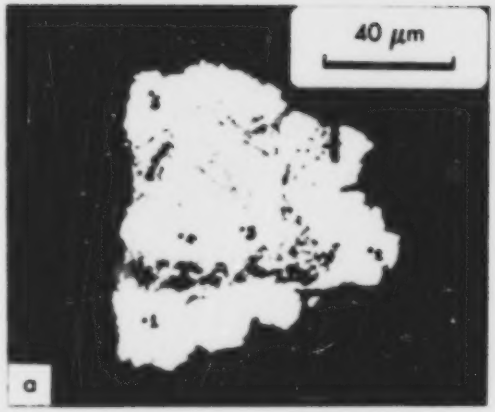

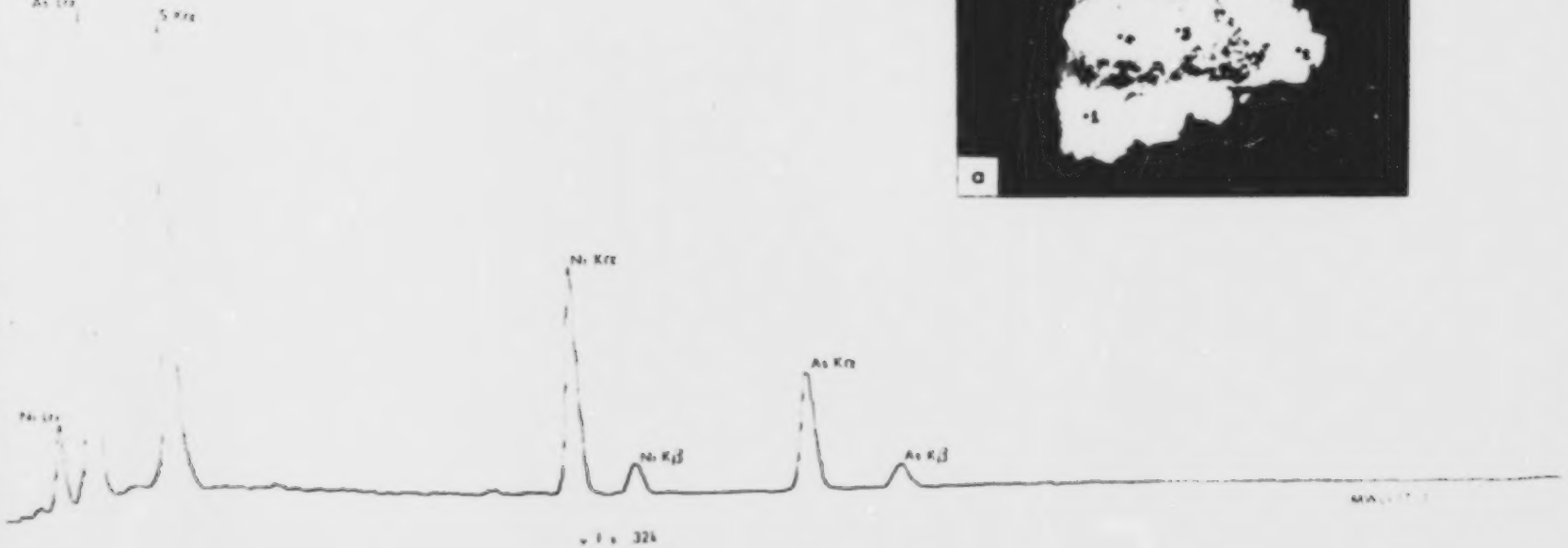

b

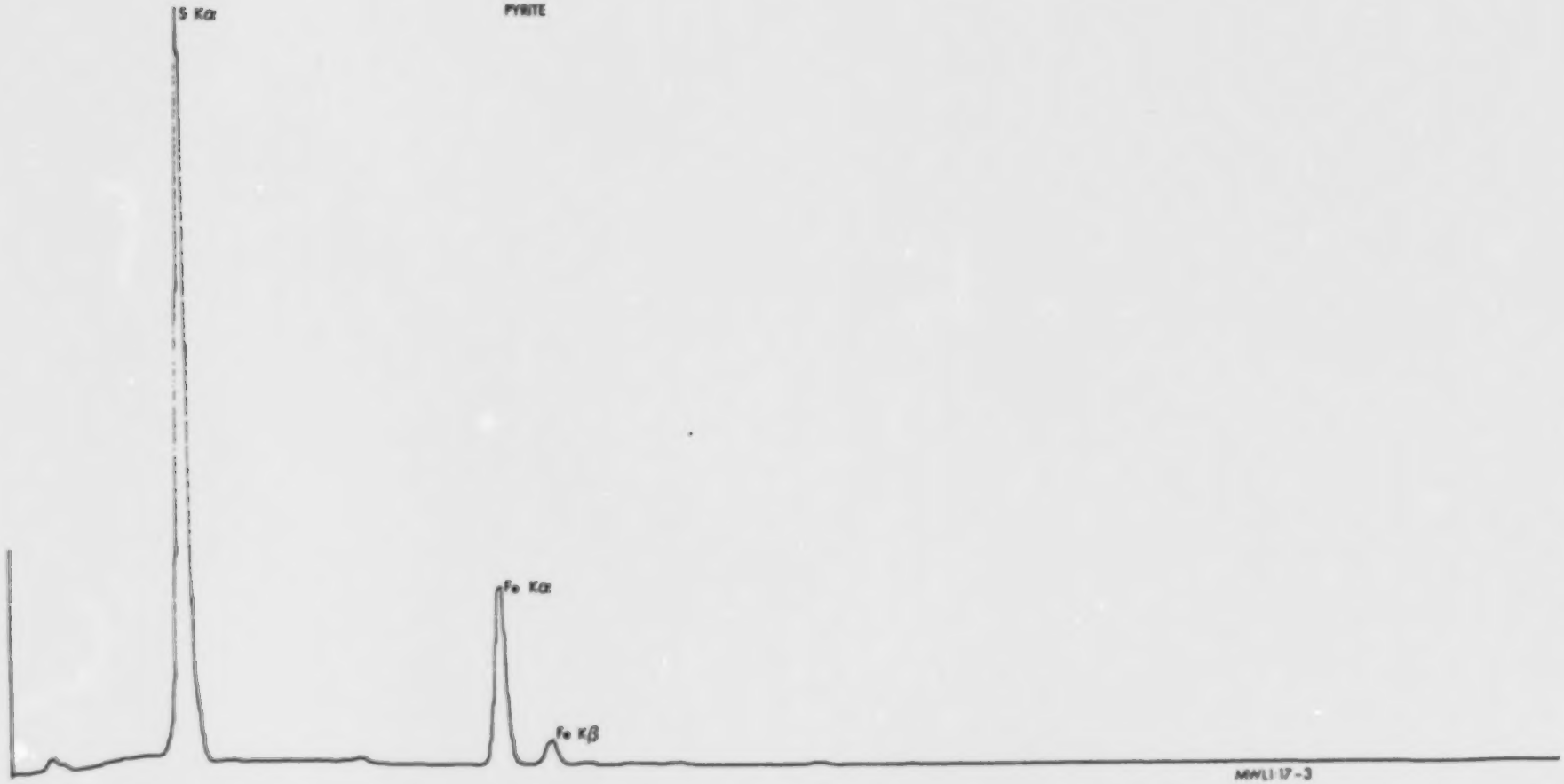

v f. s. 65k

Figure 8

(a) Sphalerite grain contains pyrite inclusions (white) and silicate-gangue matrix intergrowths (dark grey).

(b) X-ray spectrum of sphalerite.

(c) X-ray spectrum of pyrite inclusion.

SPHALERITE

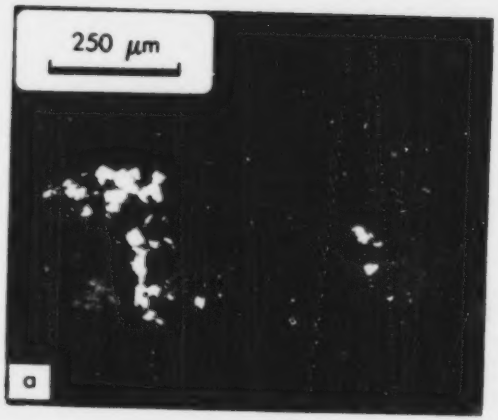

b

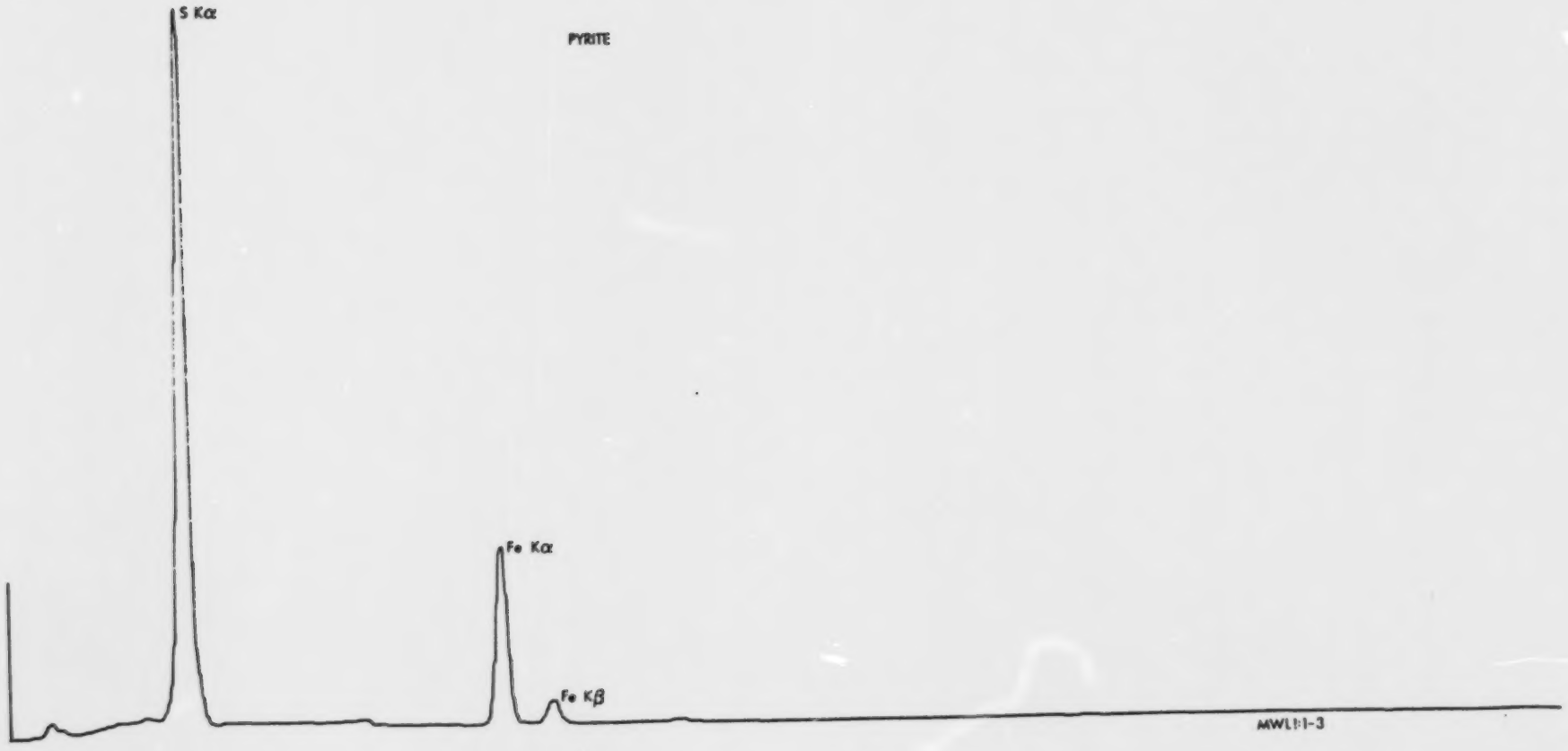

v.f.s. 65k

C

Figure 9

(a) Zircon grain exhibits chemical zoning.

(b) X-ray spectrum of zircon.

(c) X-ray spectrum of dark-grey zone in zircon grain.

ZIRCON

b

Y-RICH PHASE

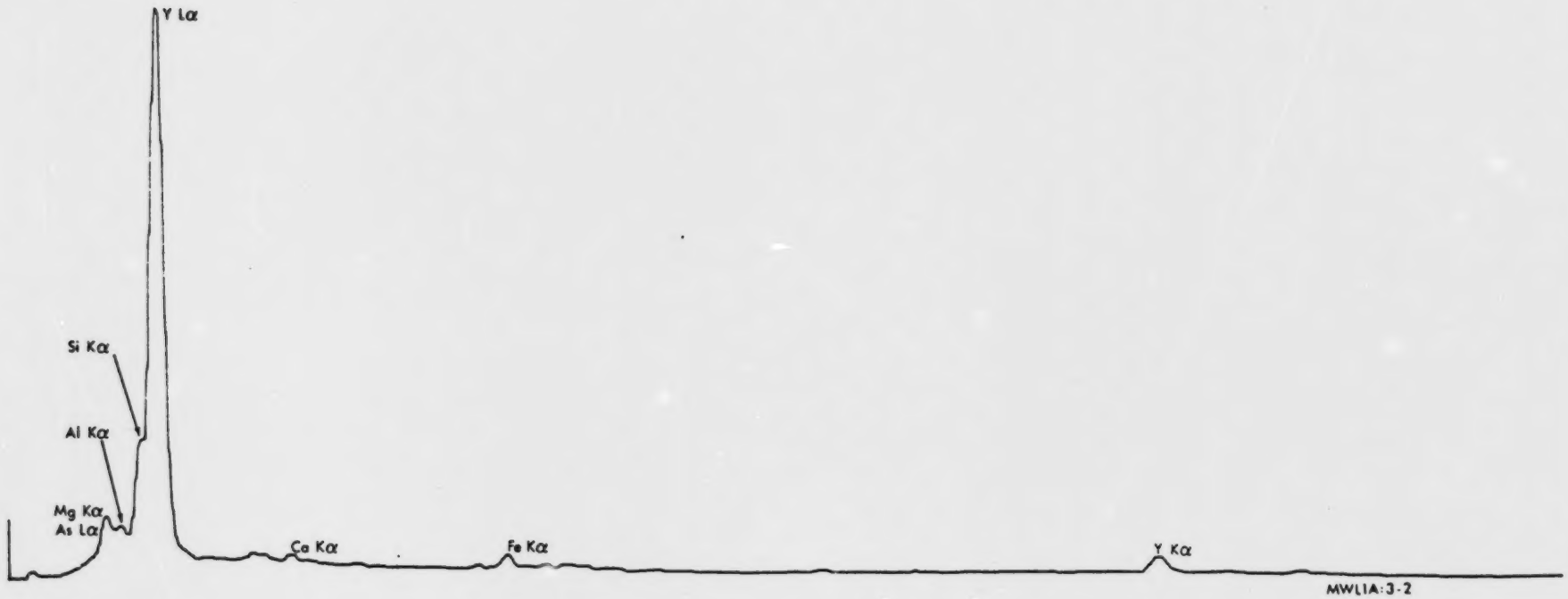

v. f. s. 32k

C

Figure 10

(a) Zircon grain displays chemical zoning.

(b) X-ray spectrum of zircon.

(c) X-ray spectrum of dark-grey zone.

ZIRCON

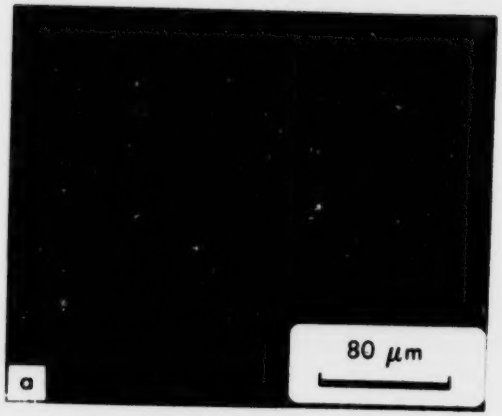

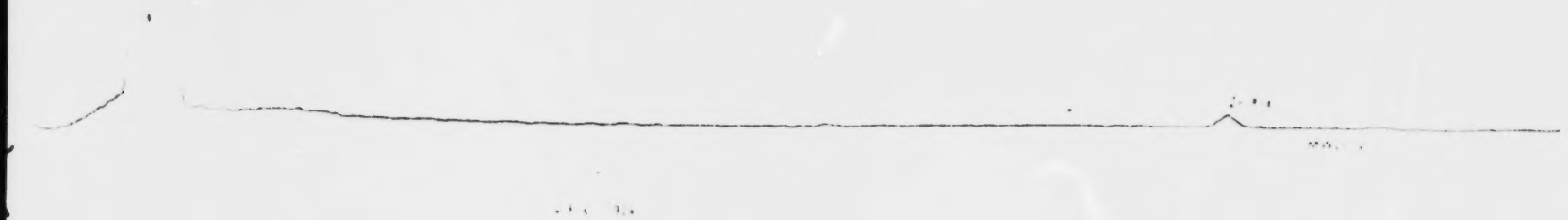

b

ZIRCON

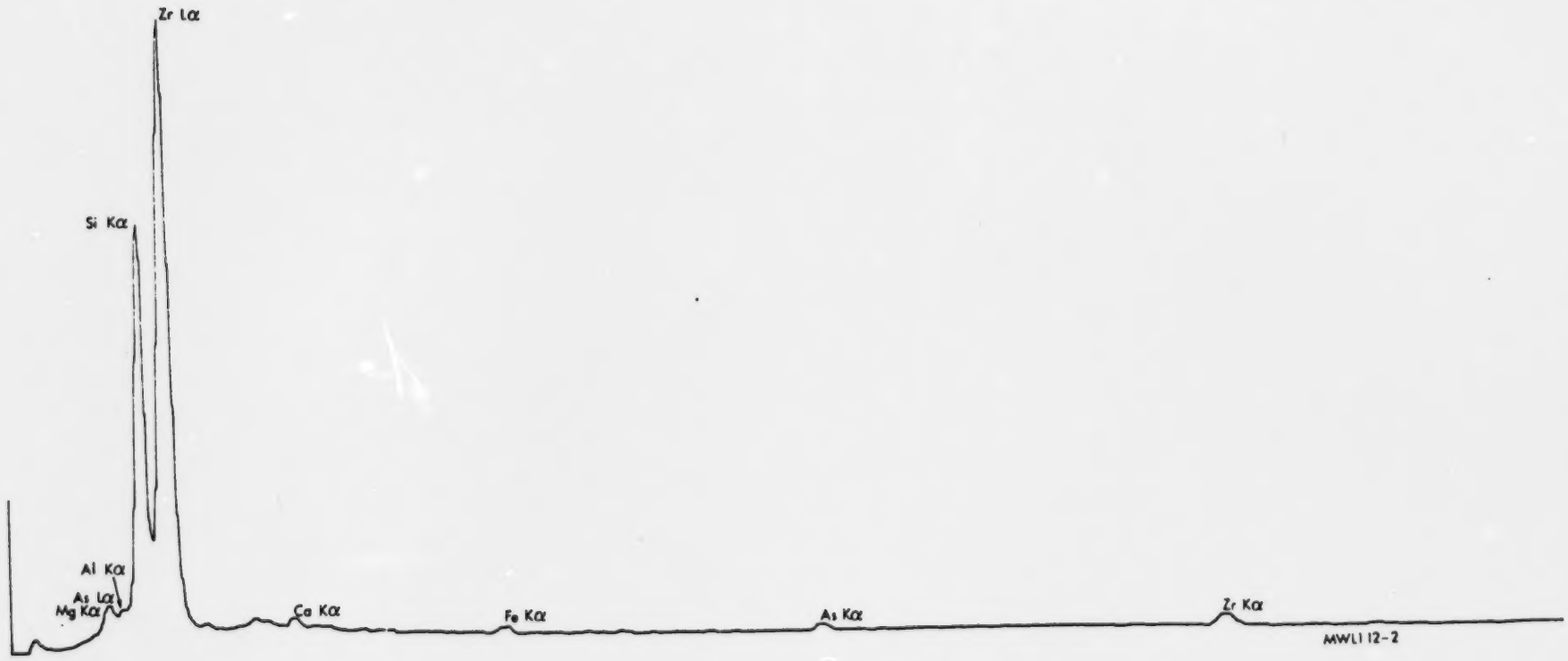

v. f. s. 32k

C

Figure 11

(a) Fractured titania grain.

(b) X-ray spectrum of titania.

TITANIA

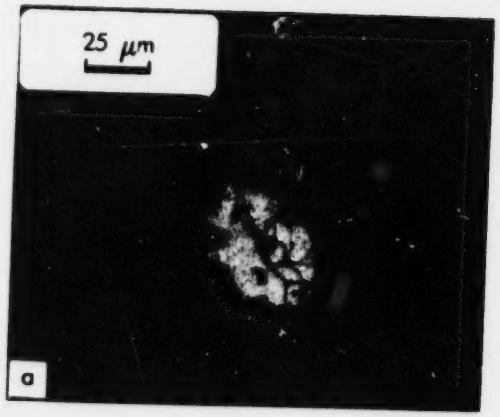

b

4. EXAMINATION OF SAMPLE SURFACES

Occurrences of all of the gangue minerals were observed in the leach residues, gersdorffite being the most abundant. Unleached and partly-leached pitchblende and coffinite were also in evidence, and their presence has been recorded by autoradiography.

The autoradiographs (Figure 12) illustrate the great abundance of pitchblende and coffinite in the unleached ore sample. The $FeCl_3$ (MWL-2) and H_2SO_4 (MWL-5) leaches were evidently the most effective in dissolving the ore minerals, as indicated by the virtual absence of discrete, high-intensity radioactive centres from the autoradiographs. However, it is readily evident in Figure 12 that the H_2SO_4 leach-residue (MWL-5) displays uniformly distributed, low-intensity radioactivity. An electron scan of part of Sample MWL-5 (Figure 13a) provides no evidence of a coating which might have accounted for the radioactivity. The tiny, white particles in area A (Figure 13a) are presented at higher magnification in Figure 13b and appear to be inclusions. In Figure 13c an electron micrograph of part of the surface of the unleached ore illustrates similar tiny, white particles which are deduced to be inclusions. Hence, those shown in Figure 13a are similarly deduced to be inclusions and not deposits formed during leaching. Consequently, it is inferred that the uniformity of distribution of the low-intensity radioactivity in Sample MWL-5 (Figure 12) is a manifestation of a radioactive species (e.g., ^{226}Ra) which has adsorbed non-selectively onto the surfaces of the grains in the leach residue.

Samples MWL-6 and -7 exhibit a uniform distribution of low-intensity radioactivity similar to that observed in Sample MWL-5 (Figure

Figure 12

Autoradiographs of polished mounts.

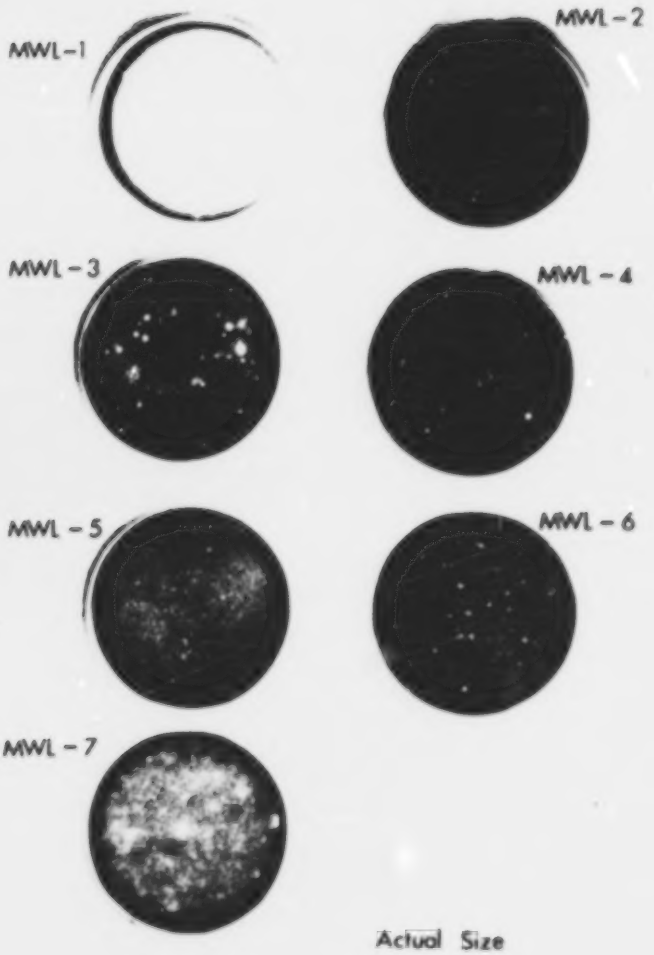

Actual Size

Figure 13

(a) Electron micrograph of MWL-5.

(b) Details of A in (a).

(c) Electron micrograph of MWL-1.

a

b

c

12). The discrete, high-intensity radioactive centres in Samples MWL-6 and -7 indicate that HNO_3 and Cl_2 respectively have been less effective than H_2SO_4 and $FeCl_3$ in dissolving the ore minerals. Figure 14a, which is a scan of part of the surface of Sample MWL-7, gives no indication of any coatings on the particles. An enlargement of area A (Figure 14a) is shown in Figure 14b which, also, does not reveal the presence of any surface coating. As with Sample MWL-5, the low-intensity radioactivity is attributed to an adsorbed species. The presence of inclusions in Figures 14a and 14b has been noted.

An electron micrograph of Sample MWL-2 is shown in Figure 15a for comparison with Figures 13 and 14. The particle, A, is depicted in greater detail in Figure 15b. No significant differences are evident among the surfaces of the particles illustrated in the three sets of micrographs.

Samples MWL-3 and -4 have yielded autoradiographs (Figure 12) which demonstrate that, unlike HCl, the $HCl-O_2$ pressure-leach has averted the adsorption of radioactive species onto the residue grains. However, the residues from both leaches contain ore minerals, which are particularly abundant in the HCl leach residue.

It is of considerable interest to note that the $FeCl_3$ and $HCl-O_2$ leach systems have been more effective than the HCl and Cl_2 systems in eluting the radioactive adsorbates. Inasmuch as they are all chloride systems, their performances differ appreciably. Possibly, the explanation of this phenomenon might involve the capability of some lixiviants as eluants of radioactive adsorbates. Wiles (1983) has described the adsorptive behaviour of some radioactive species on silicate gangue, and

Figure 14

(a) Electron micrograph of MWL-7.

(b) Details of A in (a).

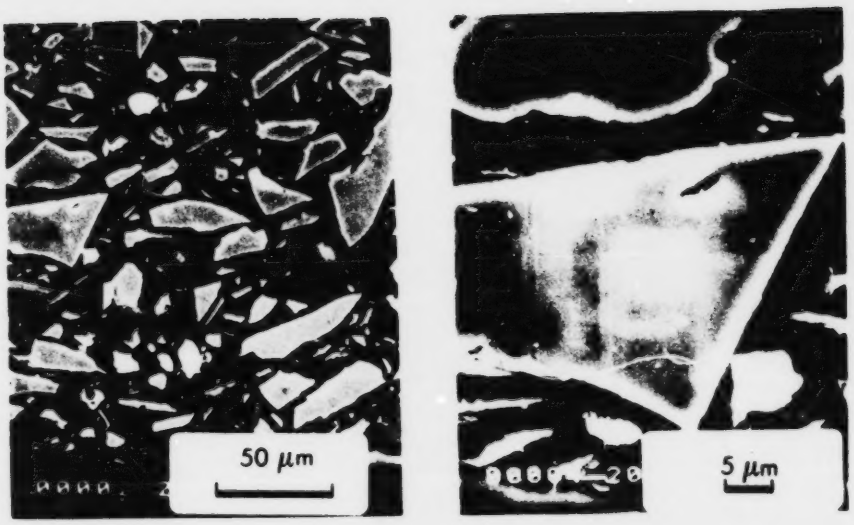

a b

Figure 15

(a) Electron micrograph of MWL-2.

(b) Details of A in (a).

a

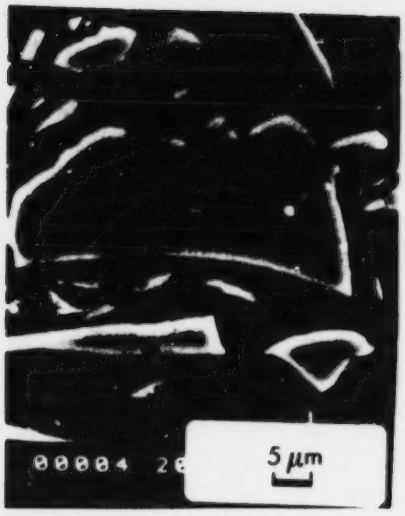

b

has alluded to the possibility that Ba^{2+} effects the elution of Ra^{2+} from Beaverlodge uranium tailings.

5. CONCLUSIONS

The findings of this work may be summarized as follows:

1. The electron micrographs have not shown any new phases to have been precipitated consequent to leaching.

2. The autoradiographs and Item #1 above, together, suggest that adsorption of radioactive species occurred on the residues from the HCl, H_2SO_4, HNO_3 and Cl_2 leaches.

3. The $FeCl_3$ leach and HCl-O_2 pressure-leach were effective in eluting radionuclides from, or in preventing the adsorption of radionuclides onto, the respective residues.

4. H_2SO_4 and $FeCl_3$ appear to have been the most effective in dissolving the ore minerals.

RECOMMENDATION

It is recommended that the use of $FeCl_3$ solutions for eluting radioactive species from Midwest Lake uranium leach-residues be investigated. The studies could include the influences of temperature, $FeCl_3$ concentration and solid/liquid ratio on the efficiency of elution. It should be equally instructive to study the viability of HCl-O_2 pressure-elution.

ACKNOWLEDGMENTS

The authors are grateful to Energy, Mines and Resources Canada for financial support for this project.

We are particularly grateful to Mr. G.M. Ritcey and Dr. K.E. Haque of CANMET for comprehensive discussions on the project.

The opportunity to exchange ideas with Dr. D.R. Wiles of Carleton University is greatly appreciated.

REFERENCES

BERMAN, R.M. (1957): The role of lead and excess oxygen in uraninite, Amer. Mineral., 42, 705-731.

DAHLKAMP, F.J. (1978): Geologic appraisal of the Key Lake U-Ni deposits, Northern Saskatchewan, Econ. Geol., 73, 1430-1449.

WILES, D.R. (1983): The radiochemistry of radium and thorium in uranium mine tailings, Water, Air, and Soil Pollution, 20, 99-108.

APPENDIX

Supplementary X-ray spectra are arranged in this section in the same order (with respect to the minerals) as the spectra in the text.

PITCHBLENDE I

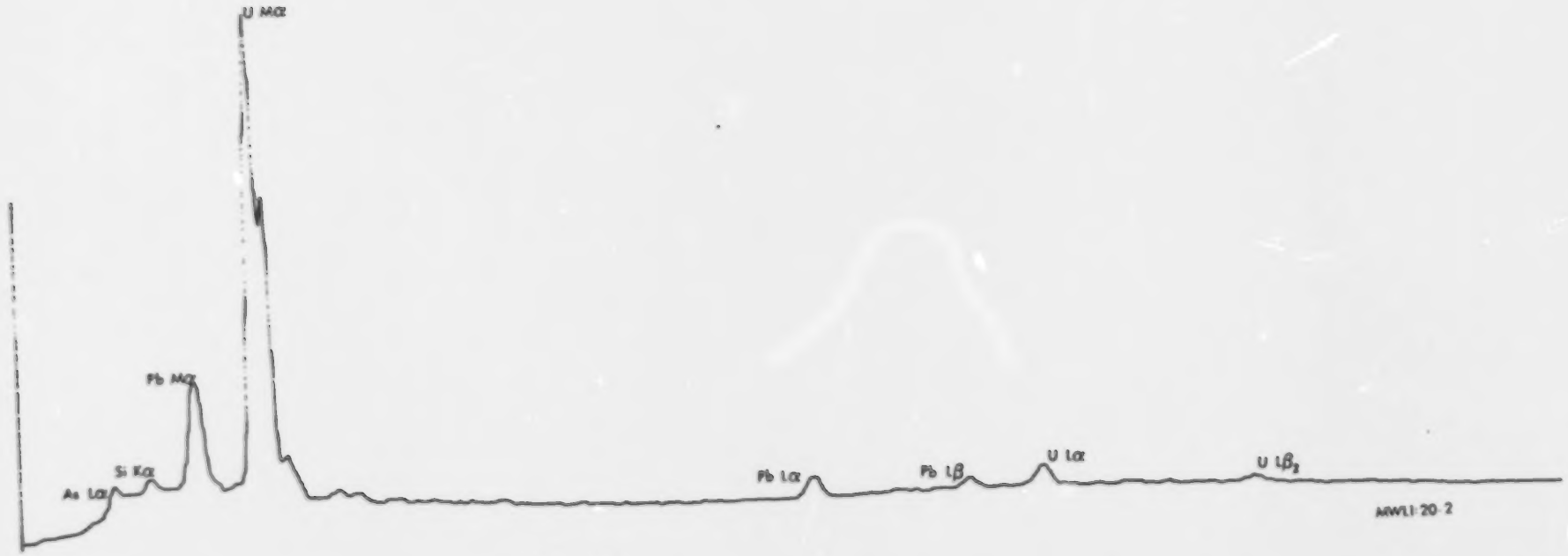

v. f. s. 32k

PITCHBLENDE II
U Mα
As Lα
Pb Mα
Si Kα
Ti Kα
As Kα
Pb Lα
As Kβ
Pb Lβ
U Lα
U Lβ2
v. f. s. 164
MWL120-4

GALENA – PITCHBLENDE II intergrowth

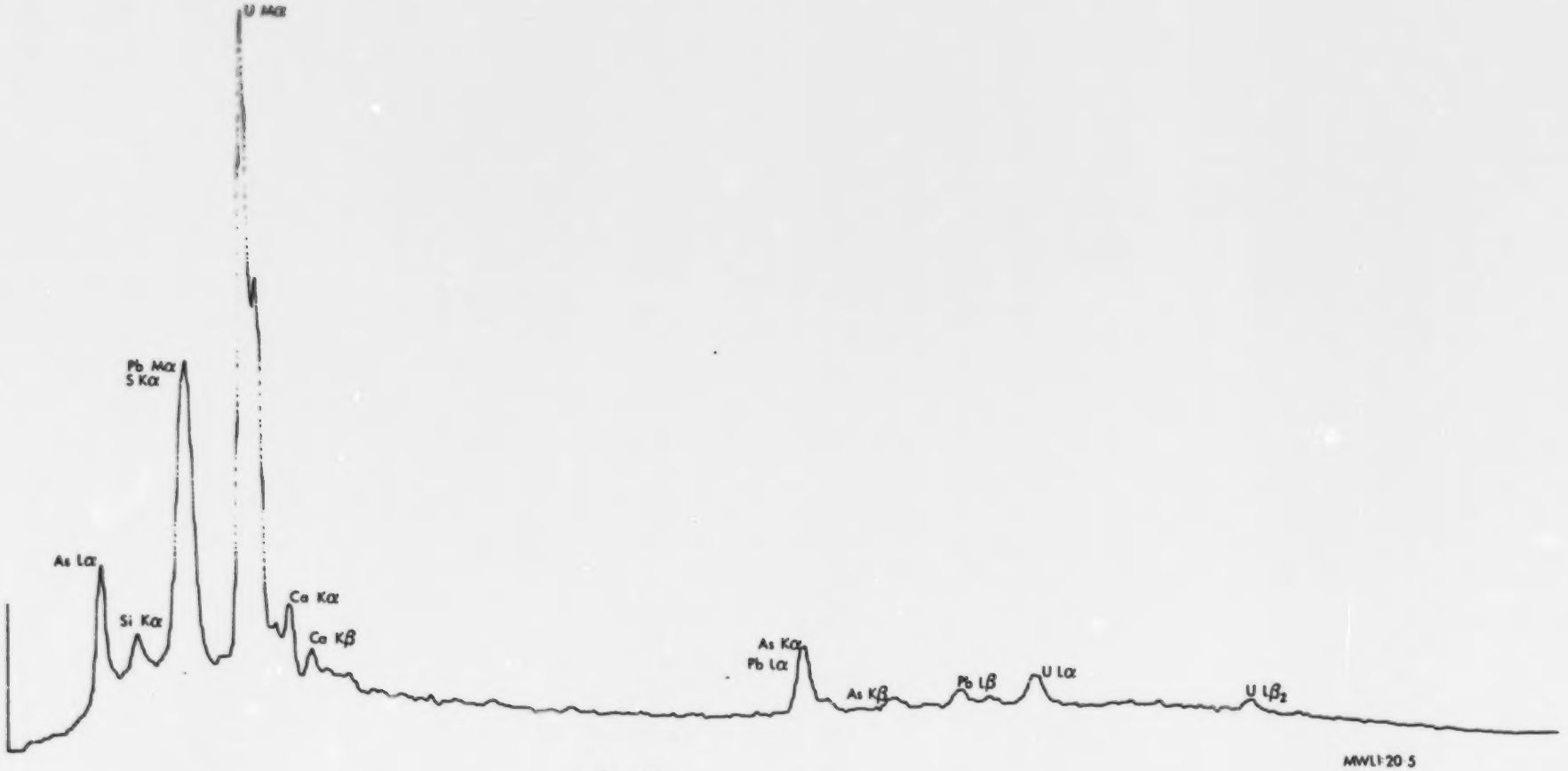

v. f. s. 16k

MWL1-20 5

PITCHBLENDE – COFFINITE intergrowth

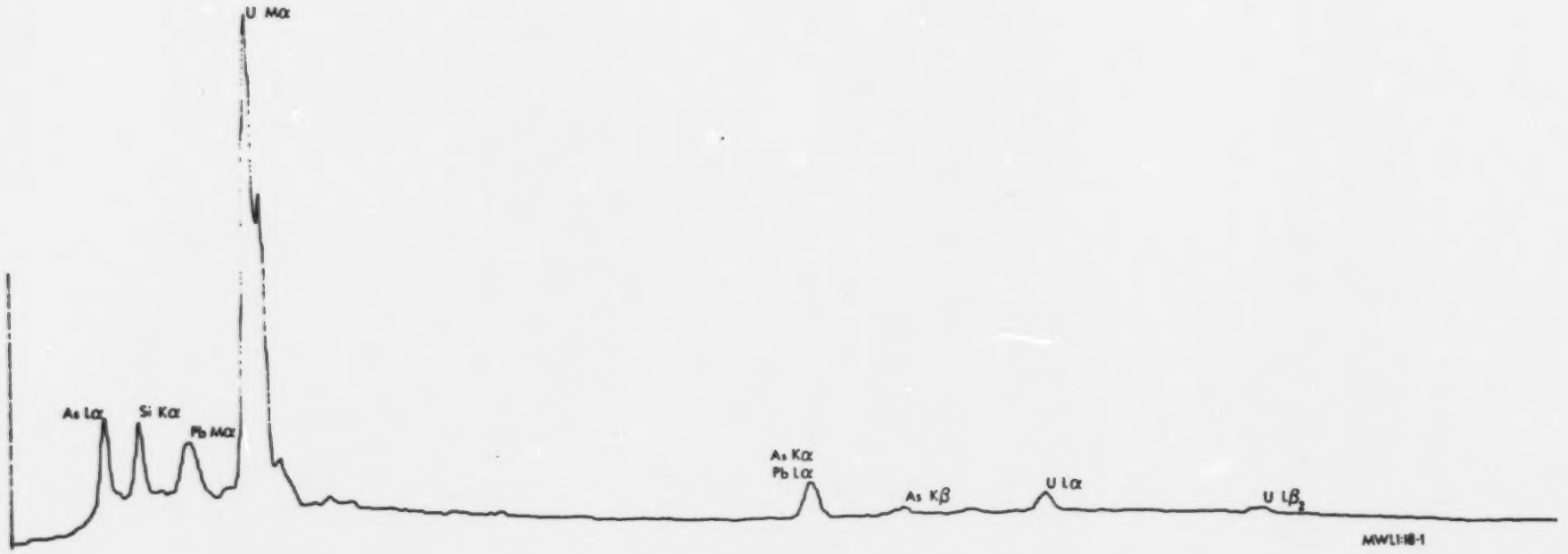

v. f. s. 32k

PITCHBLENDE I

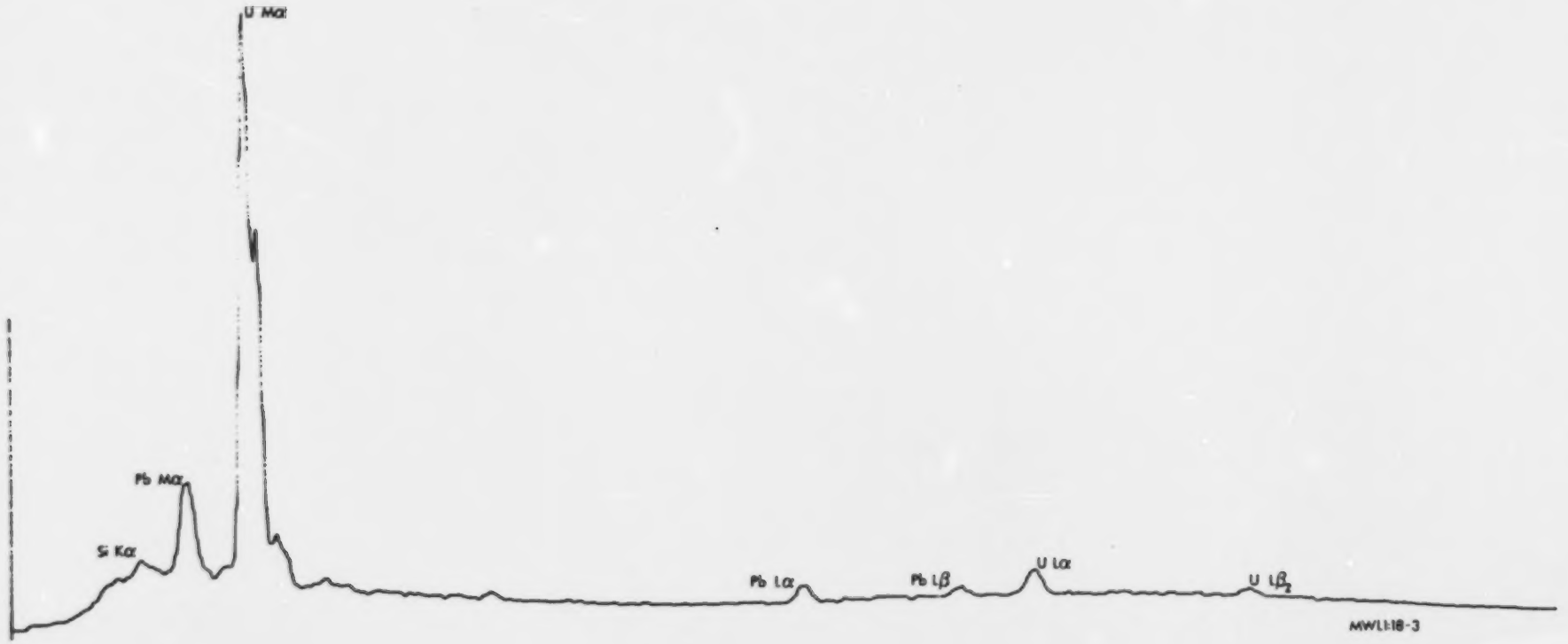

v. f. s. 32k

PITCHBLENDE – COFFINITE intergrowth with minor GERSDORFFITE

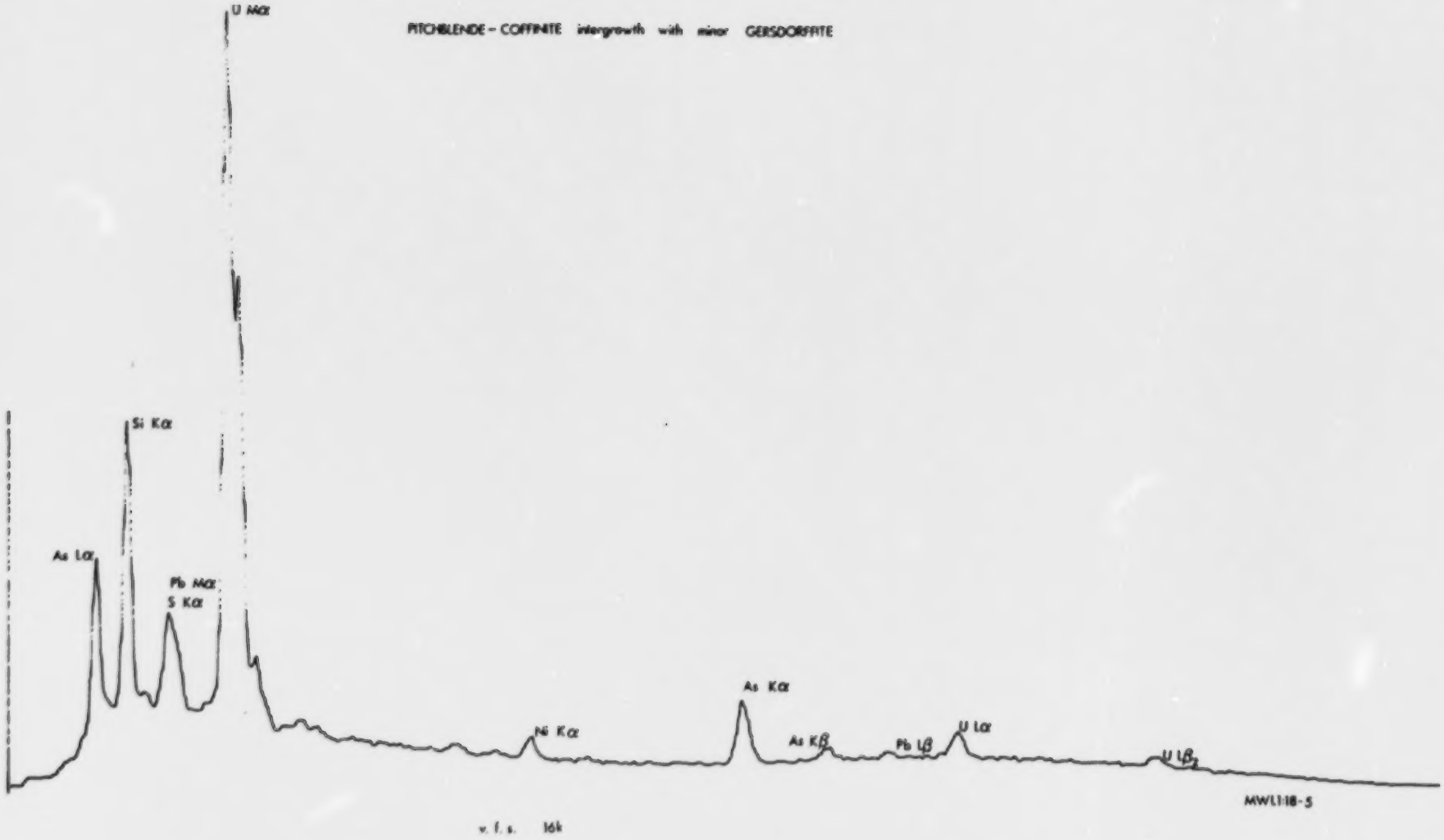

COFFINITE

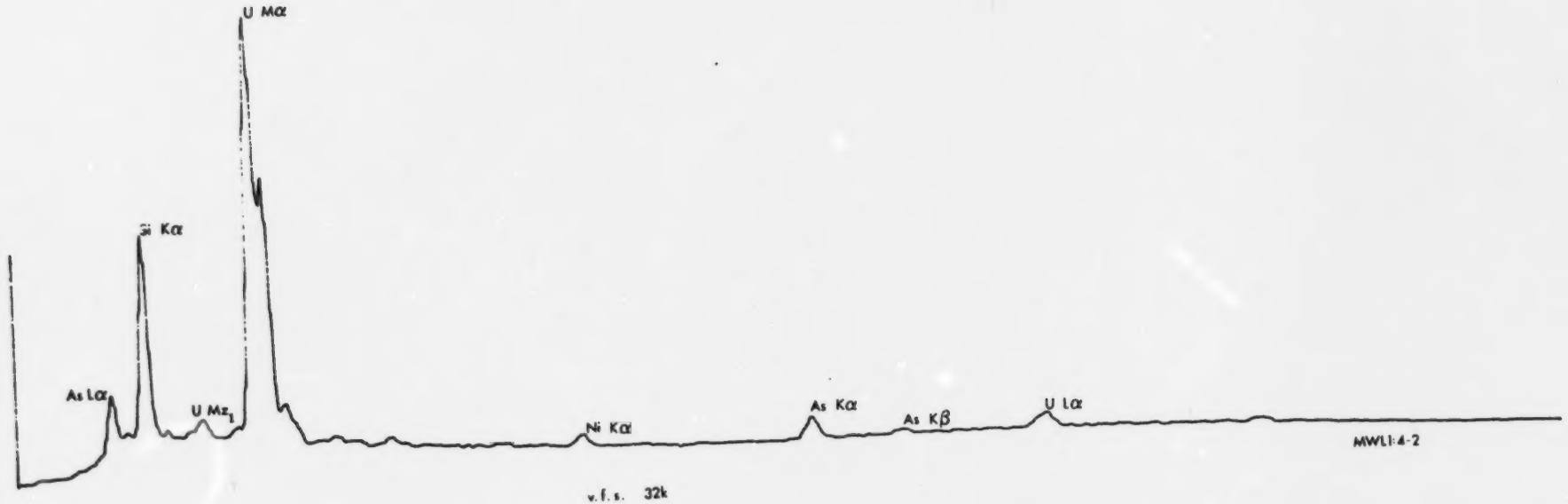

COFFINITE

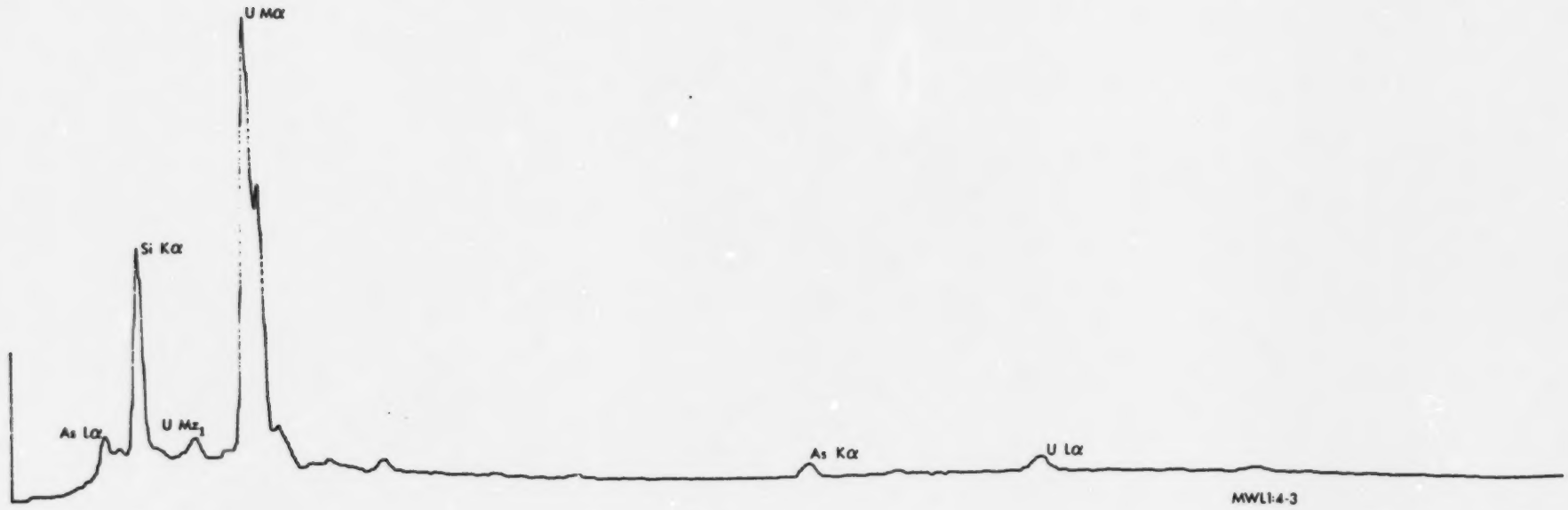

v. f. s. 32k

GOETHITE

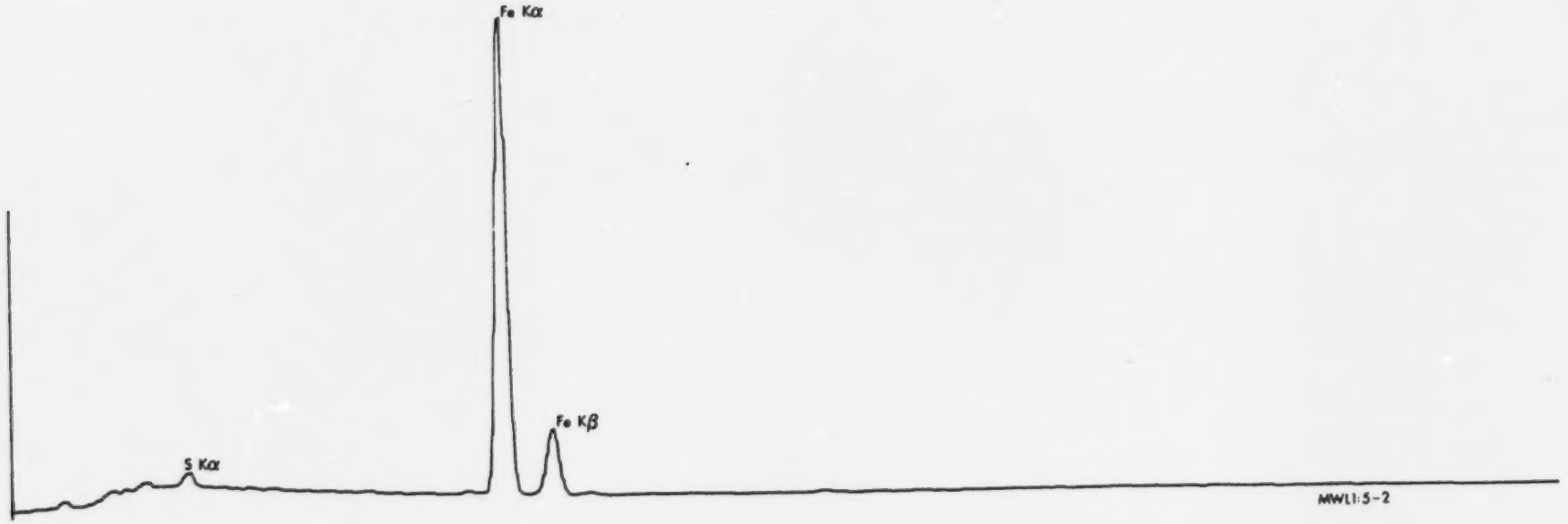

v.f.s. 32k

GOETHITE

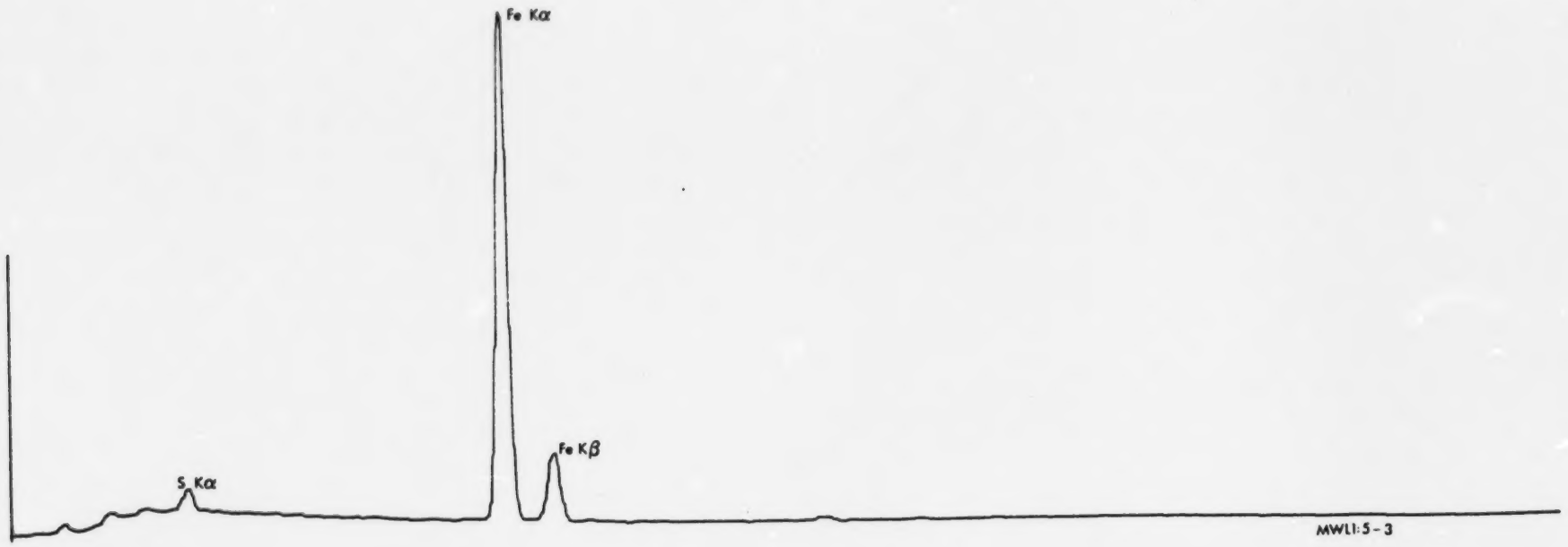

v. f. s. 32k

HEMATITE

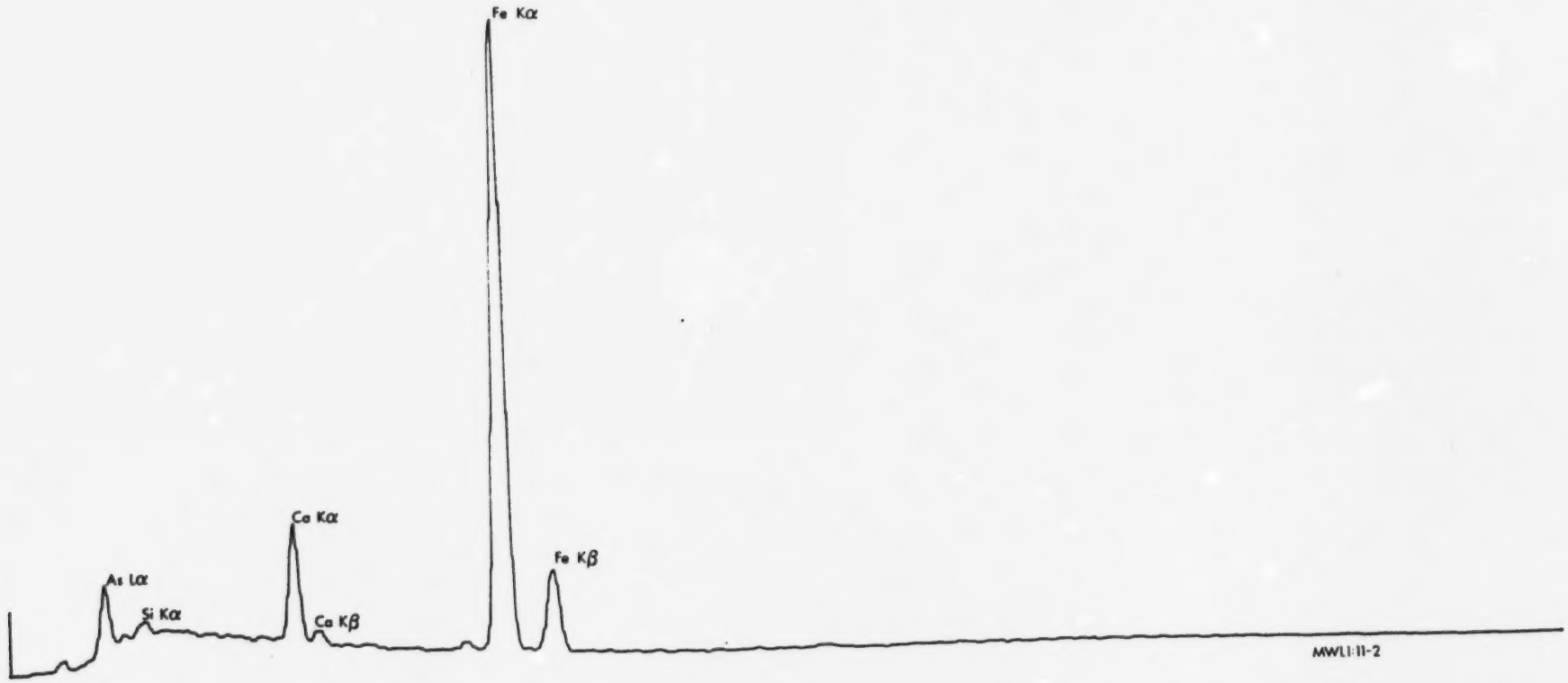

v. f. s. 16k

GOETHITE

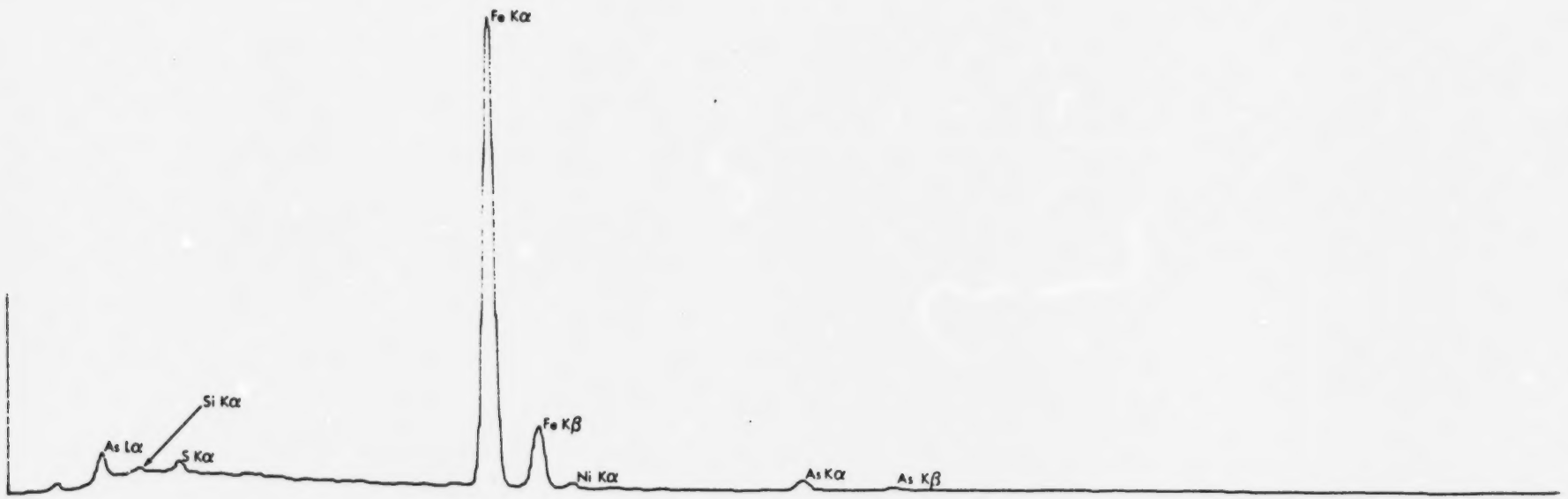

MWL1-1-2

v. f. s. 32k

GOETHITE

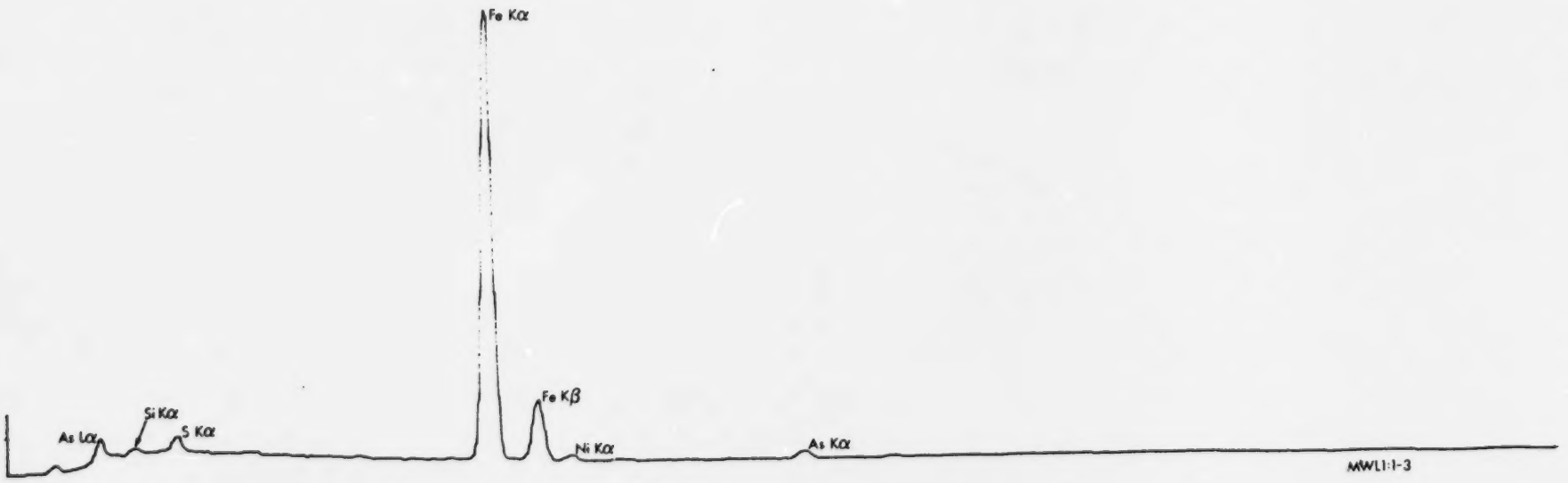

v f s 32k

MAGNETITE

v. f. s. 32k

MAGNETITE

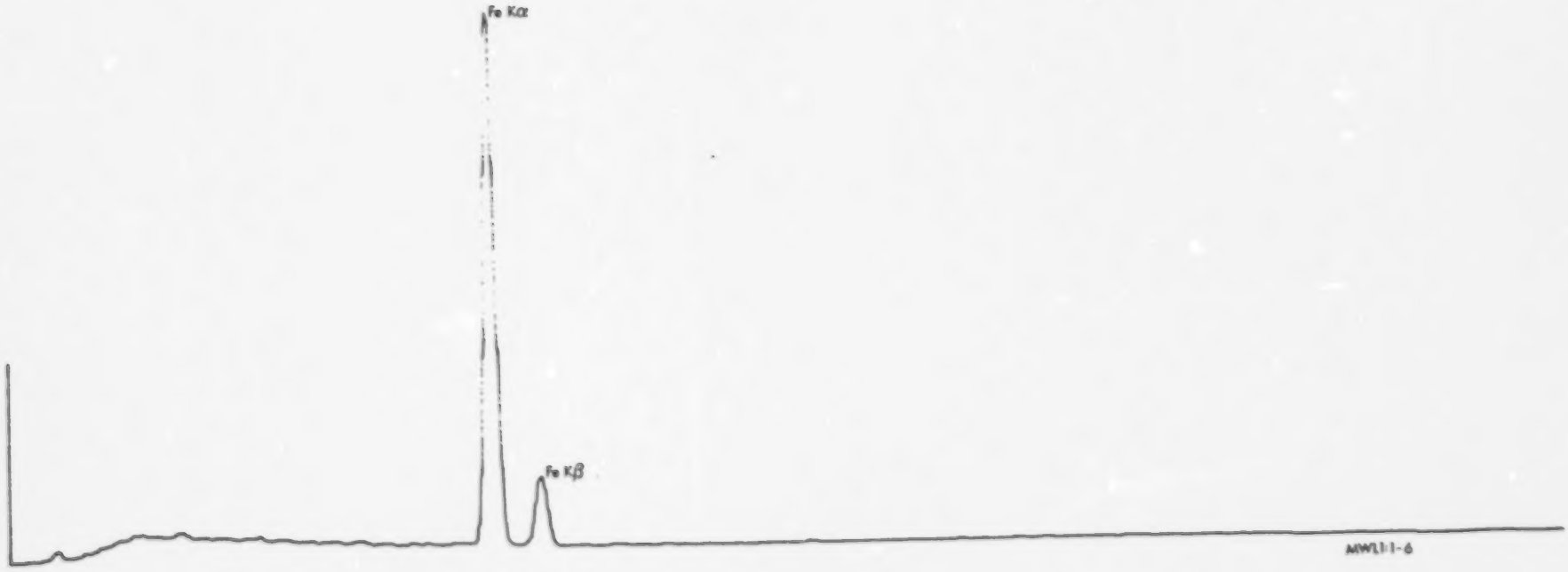

v. f. s. 32k

GOETHITE

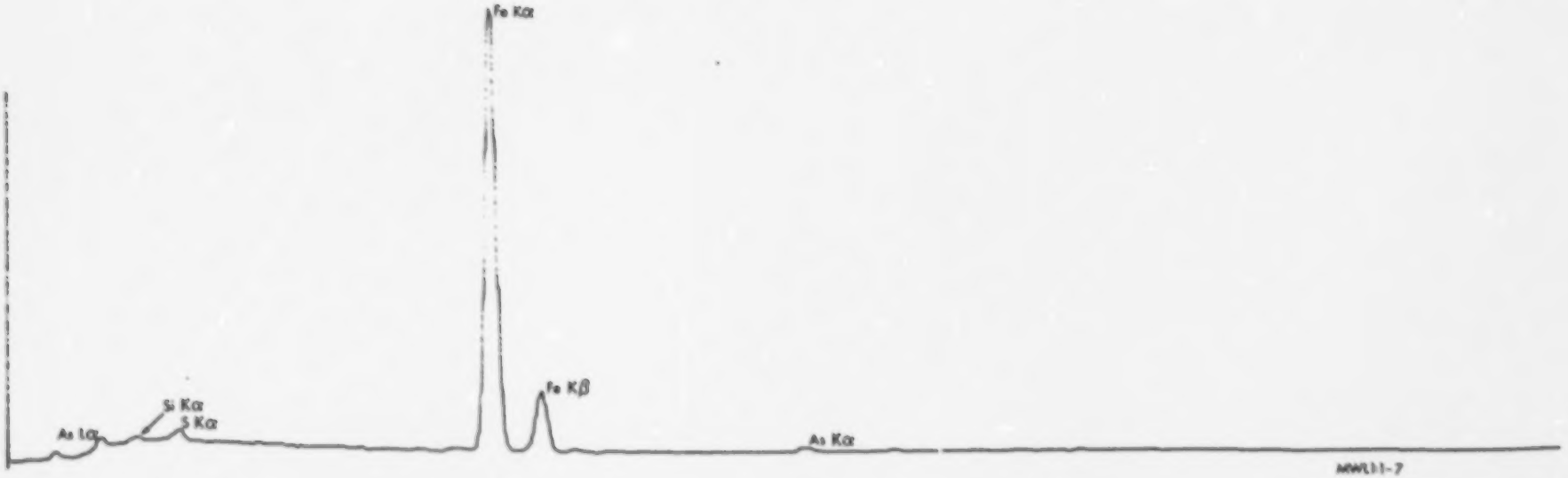

v. f. s. 32k

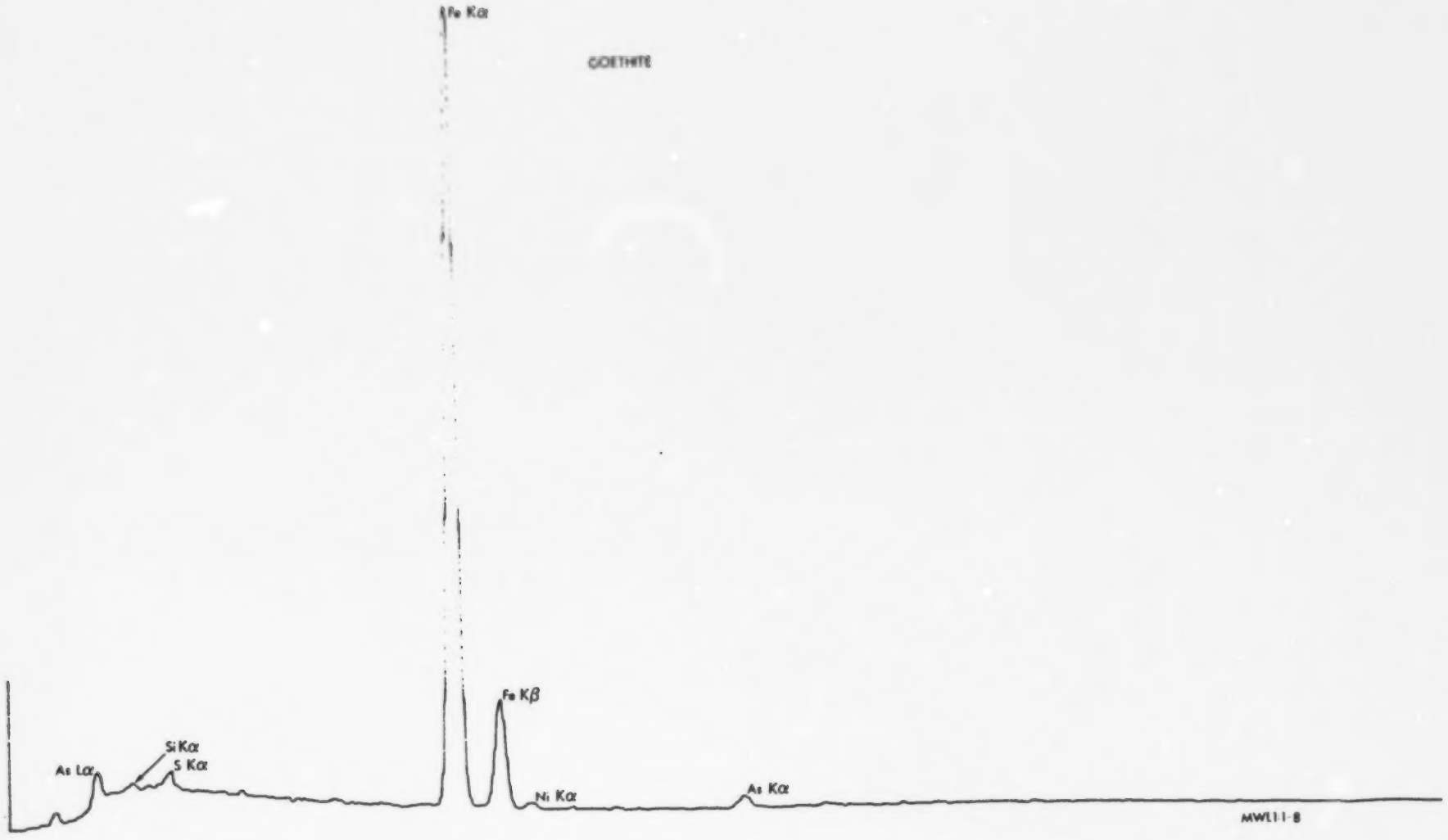
Fe Kα
GOETHITE
Fe Kβ
Si Kα
S Kα
As Lα
Ni Kα
As Kα
MWL11-8
v. f. s. 16k

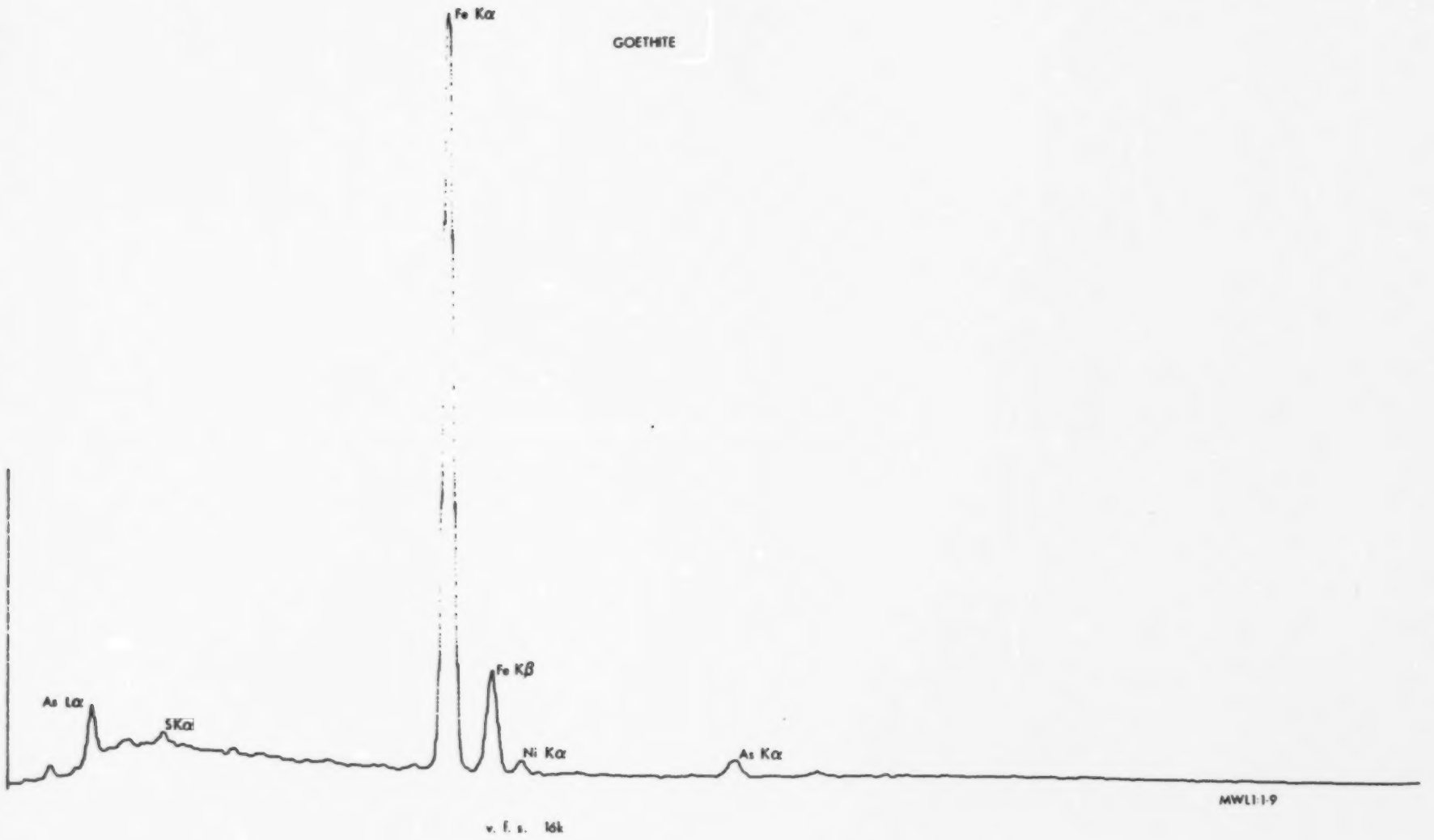
Fe Kα
GOETHITE
As Lα
SKα
Fe Kβ
Ni Kα
As Kα
MWL1-1-9
v. f. s. 16k

HEMATITE with minor GERSDORFFITE

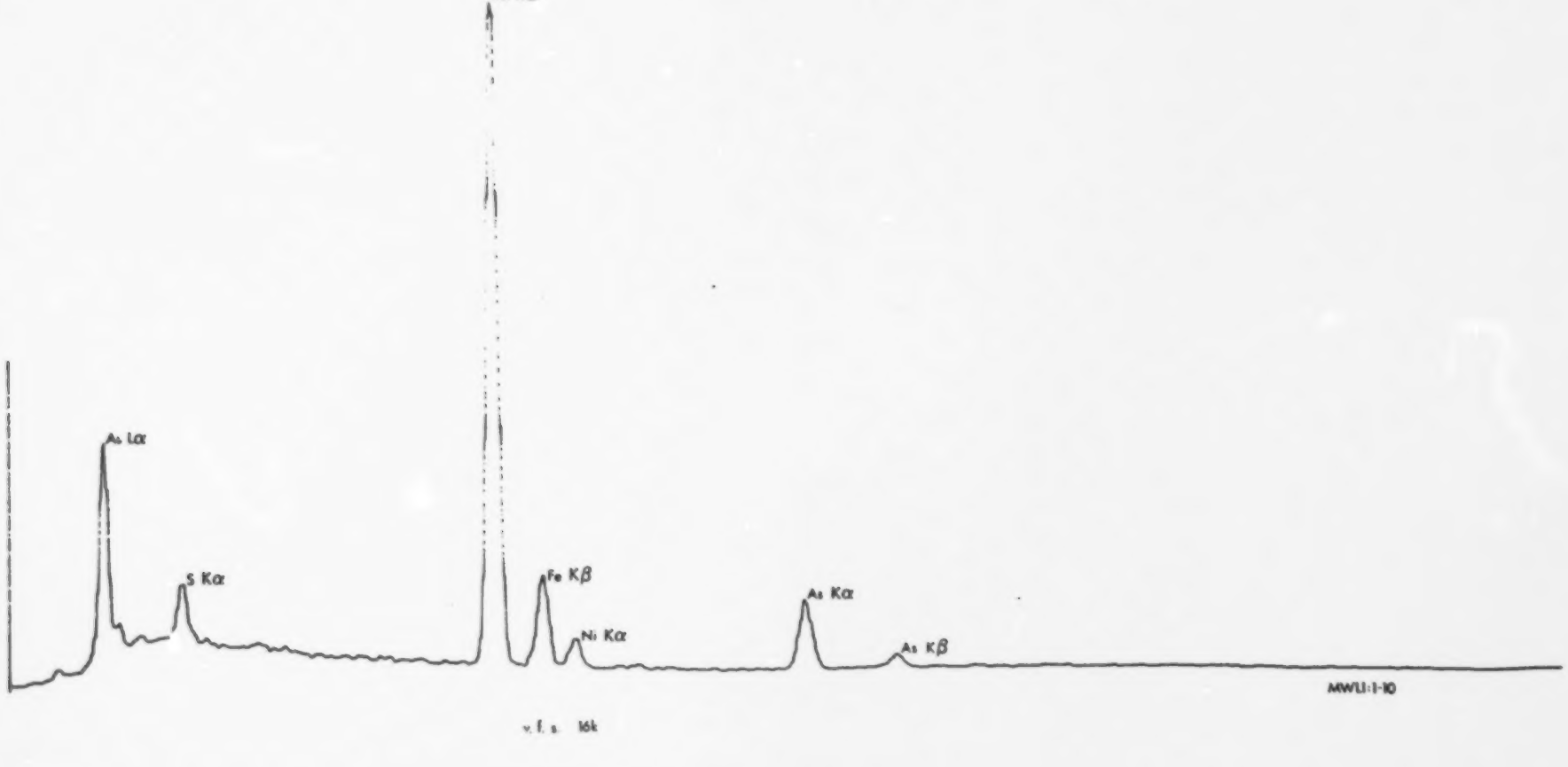

v. f. s. 16k

HEMATITE with minor GERSDORFFITE

GERSDORFFITE

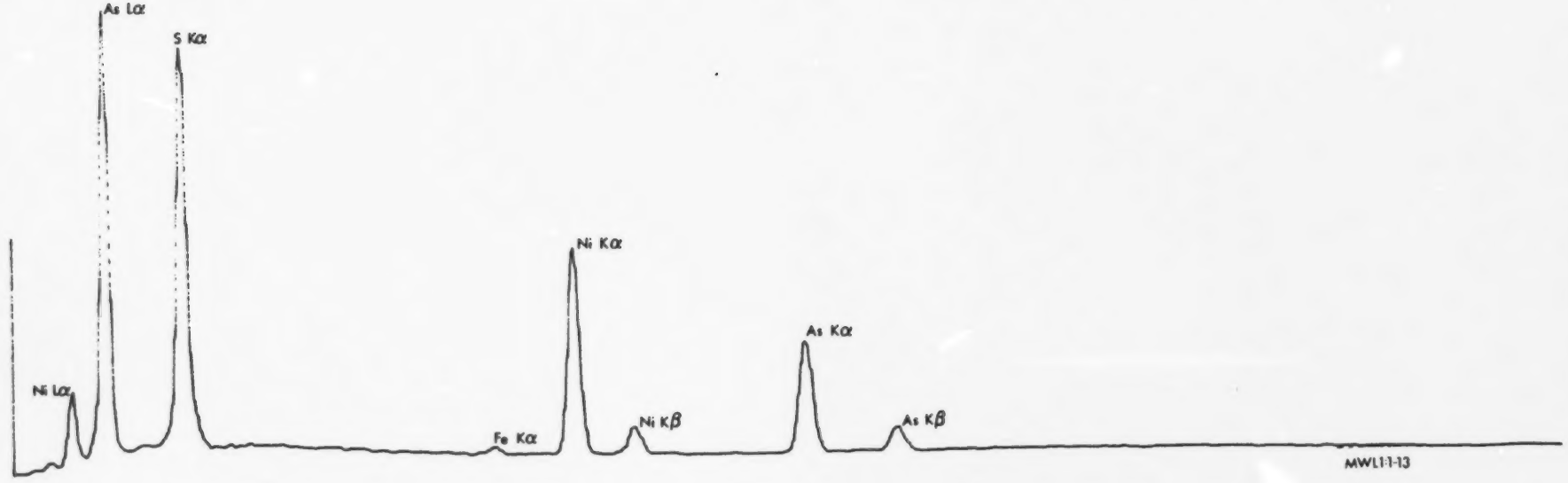

v. f. s. 32k

GERSDORFFITE

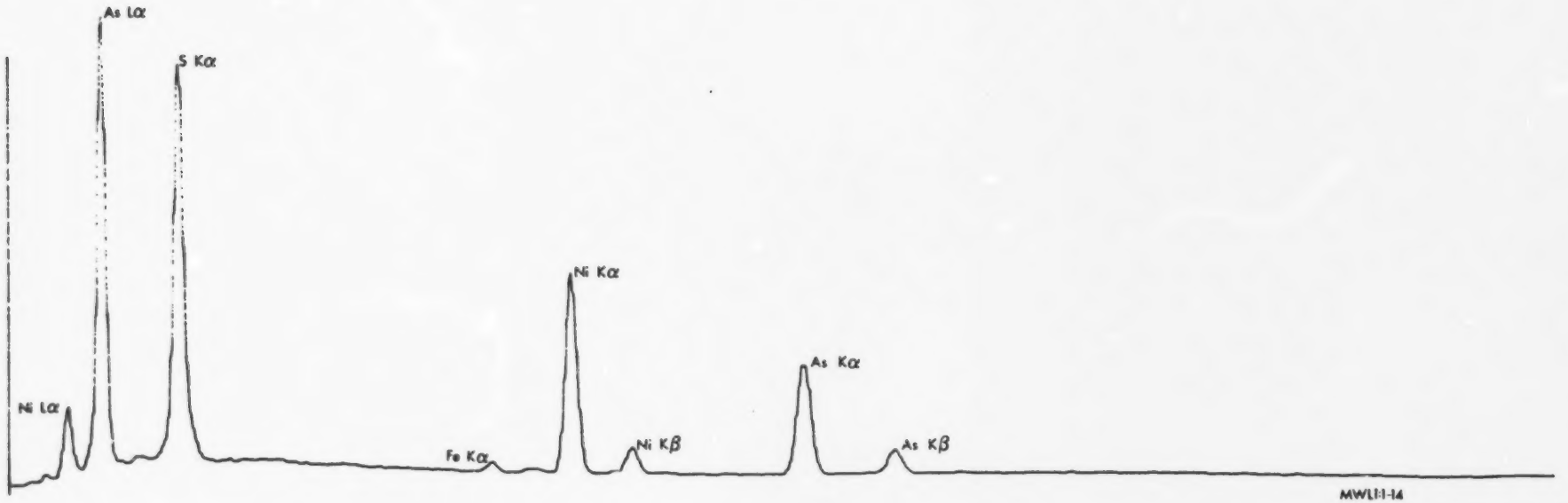

v. f. s. 32k

GERSDORFFITE

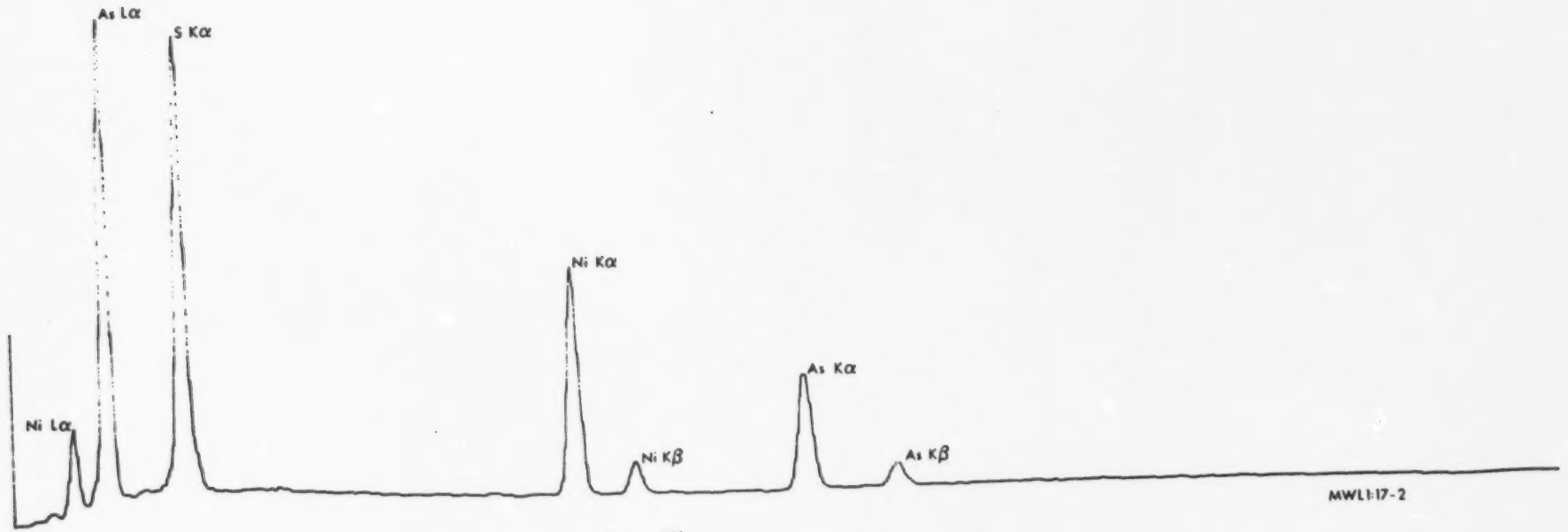

v. f. s. 32k

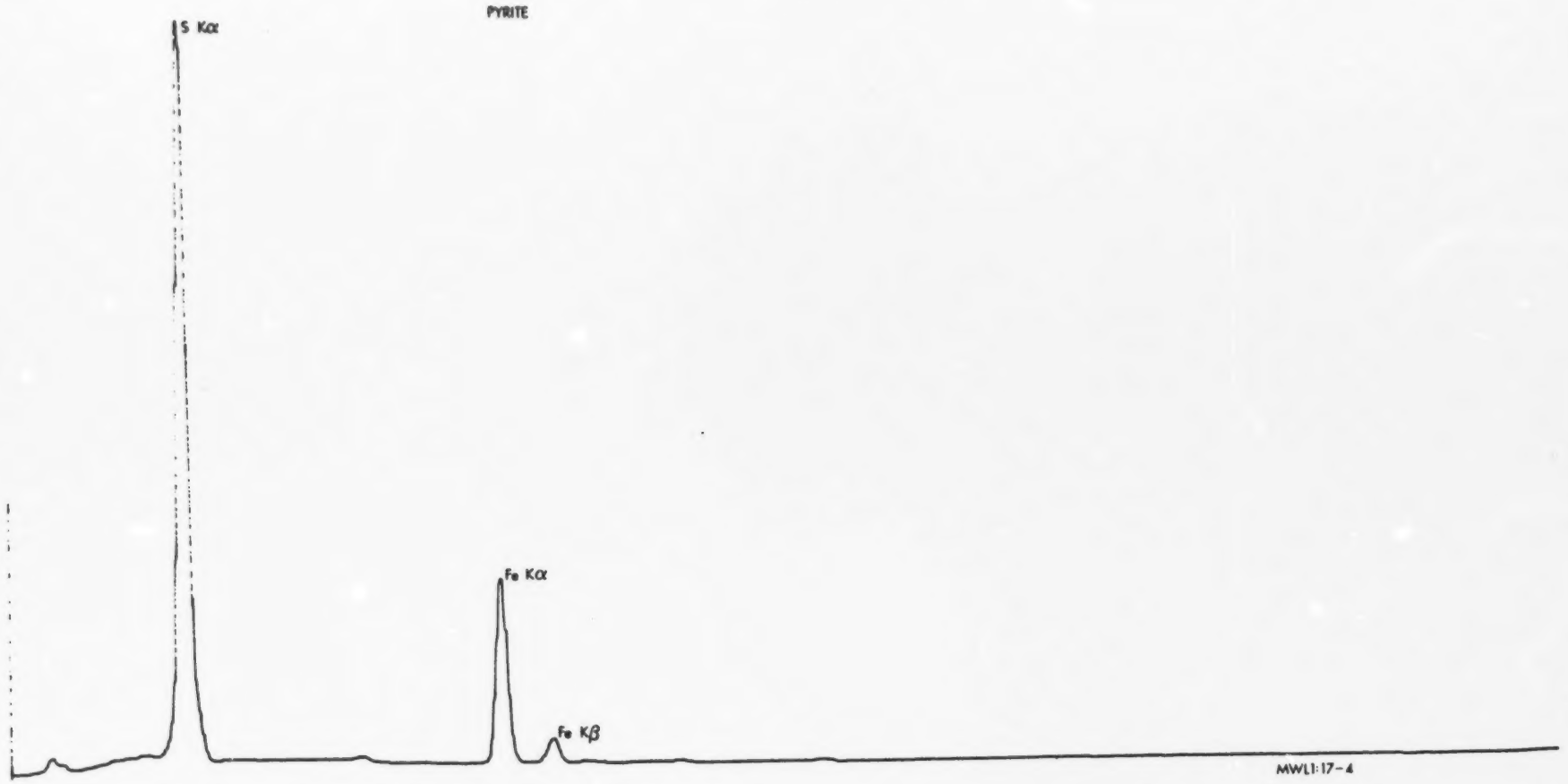

v. f. s. 65k

GERSDORFFITE

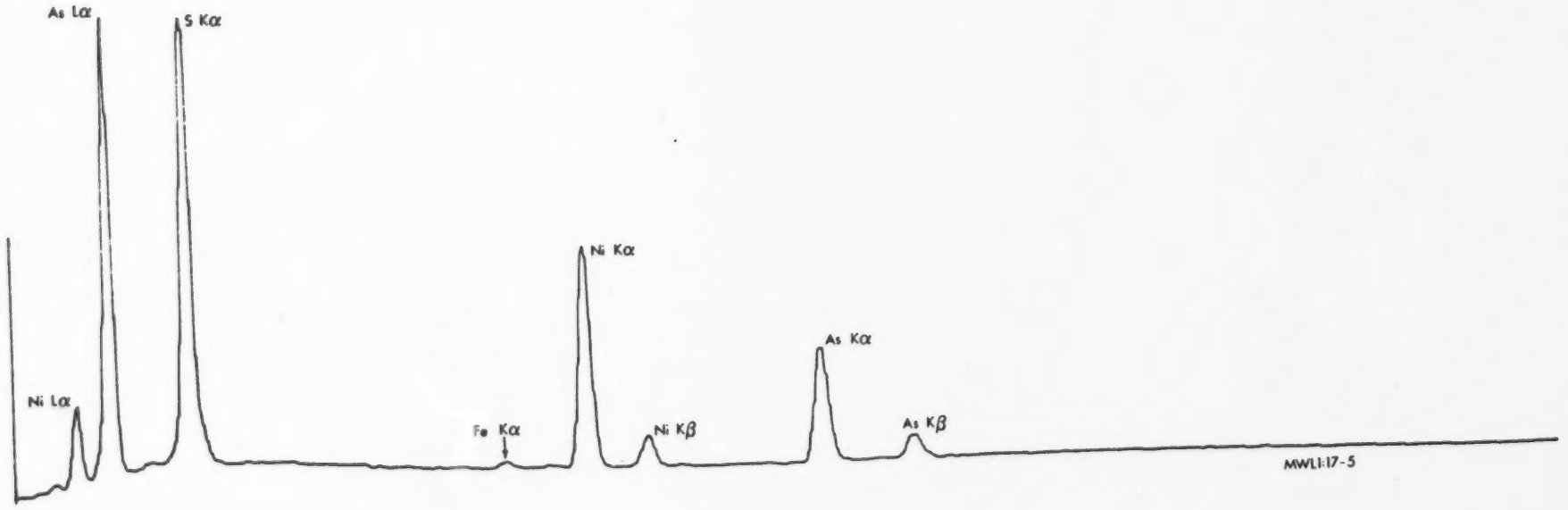

v. f. s. 32k

SPHALERITE
S Kα
Zn Lα
Zn Kα
Fe Kα
Fe Kβ
Zn Kβ
MWL1A:1-2
v.f.s. 32k

S Kα
PYRITE
Fe Kα
Fe Kβ
MWL1A 1 4
v f s 65k

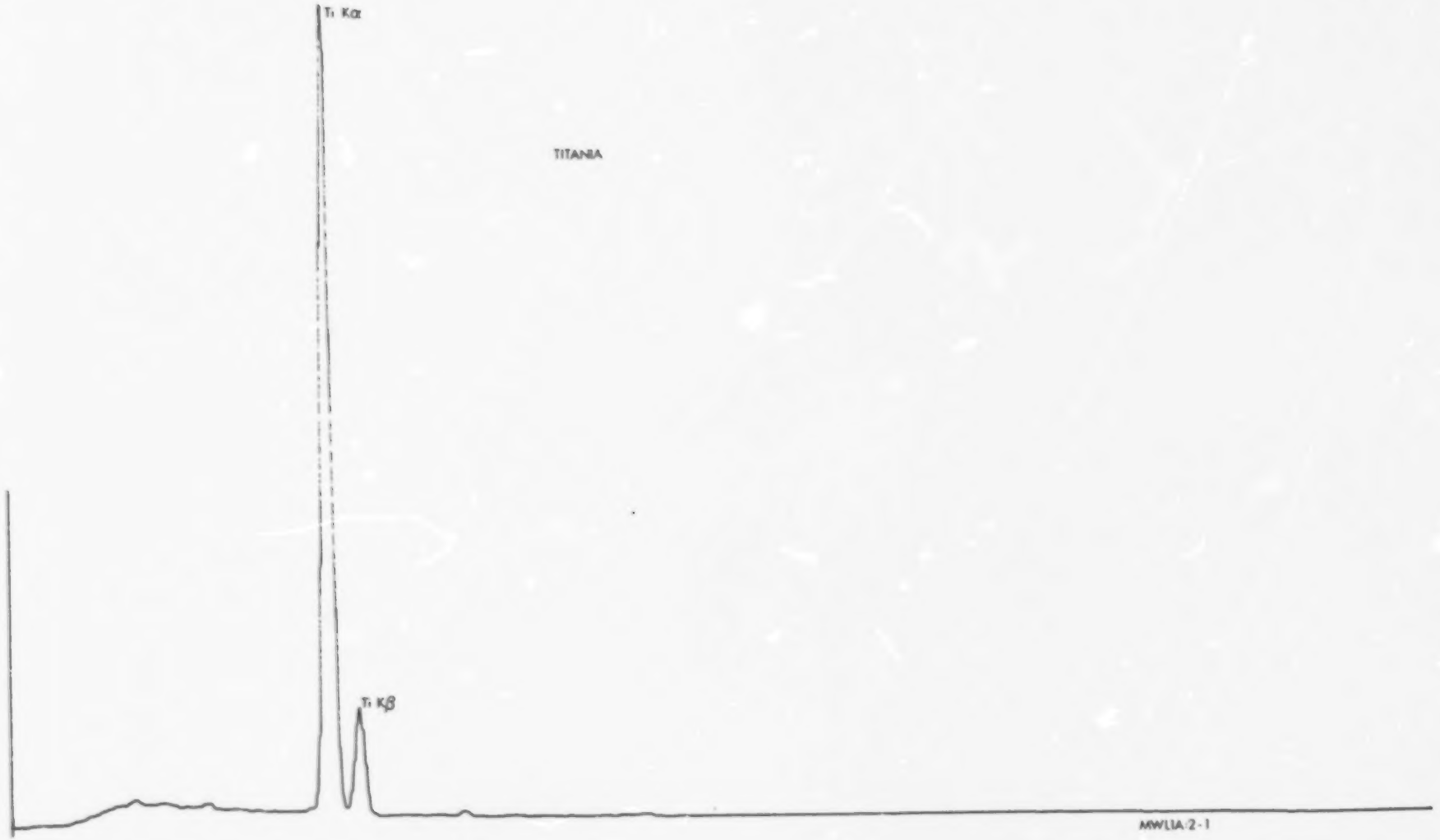

v. f. s. 32b

PYRITE

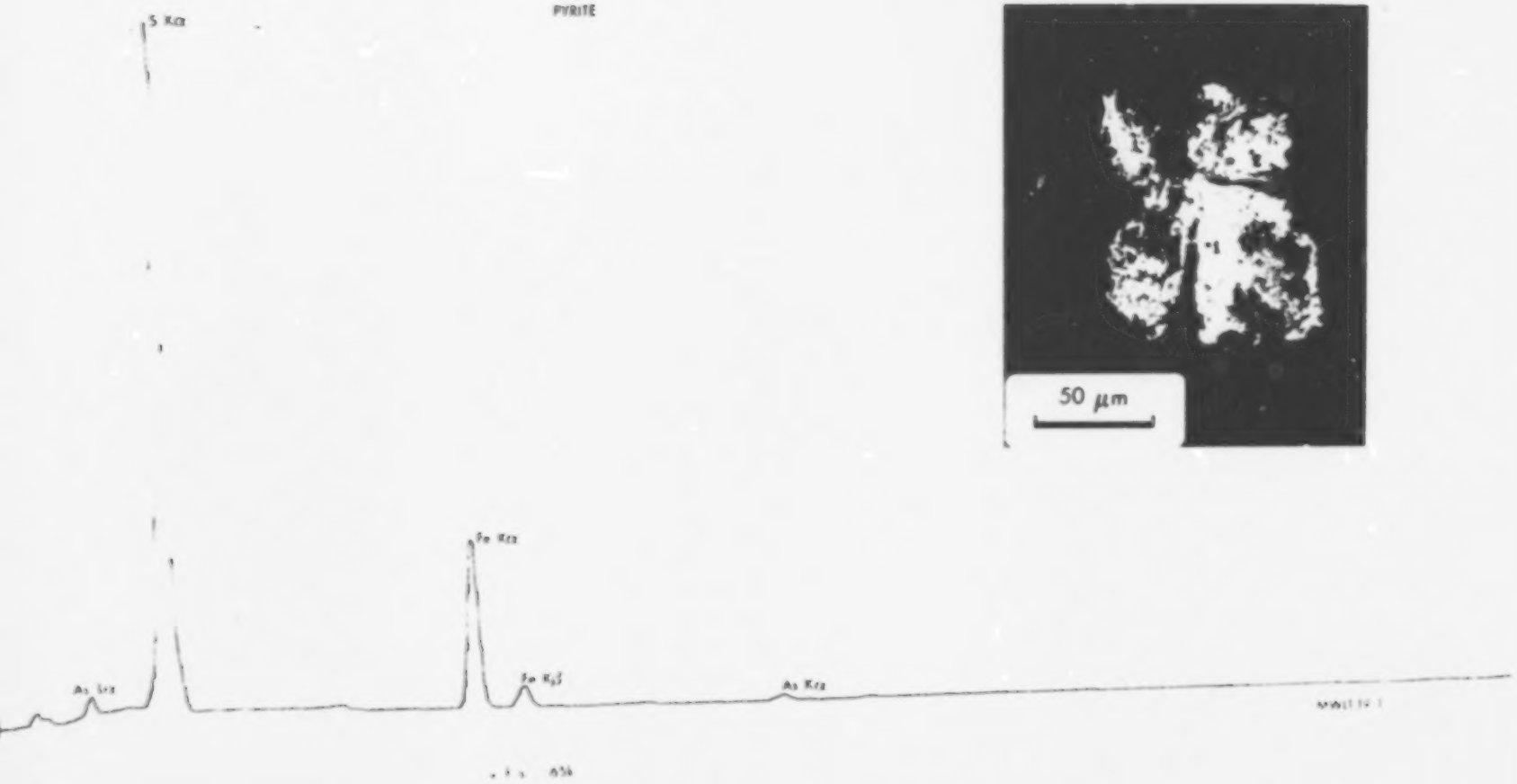

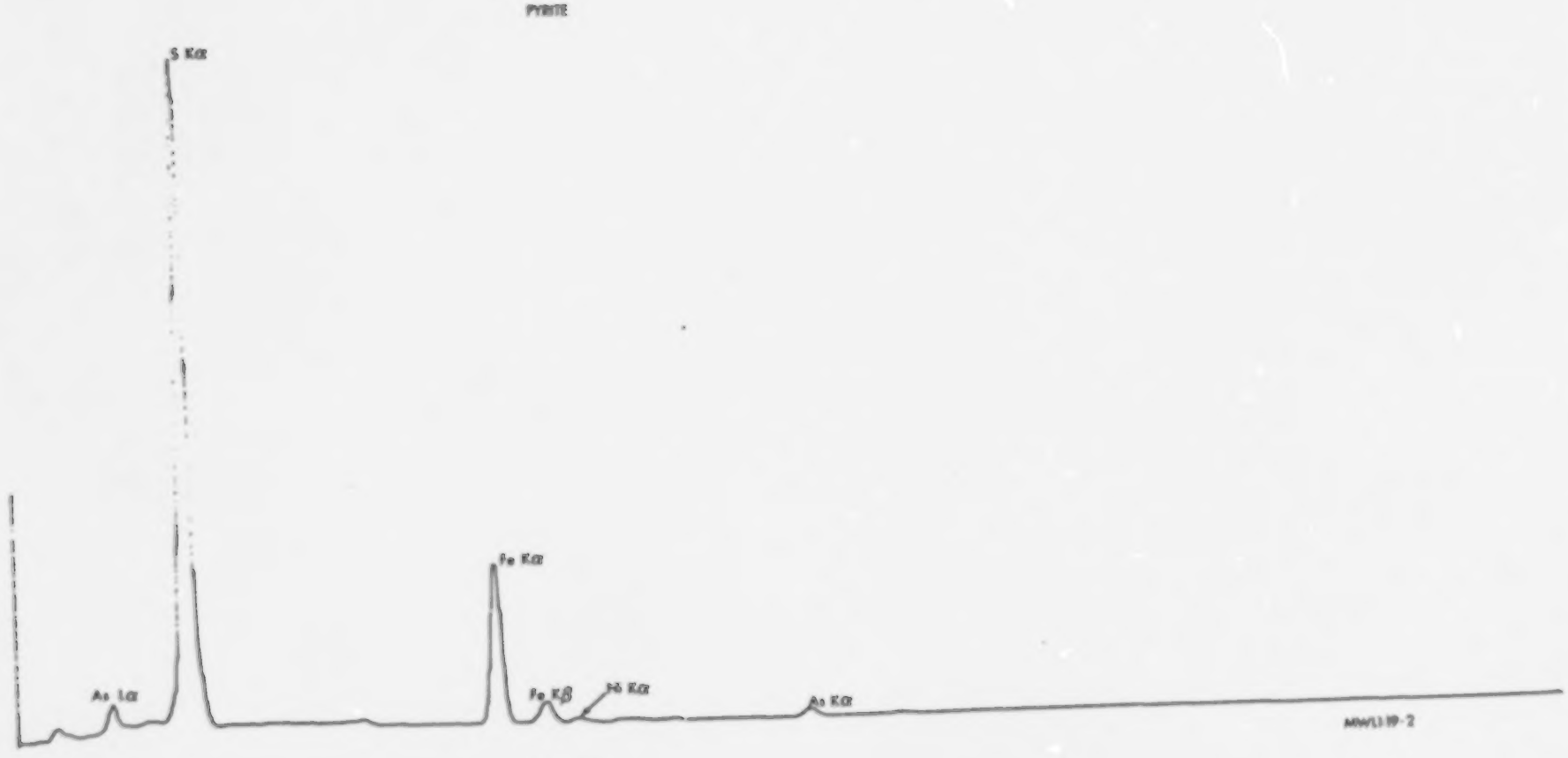
PYRITE
S Kα
As Lα
Fe Kα
Fe Kβ
Co Kα
As Kα
MNWL1 19-2
v. l. s. 65k

PYRITE - GERSDORFFITE - GALENA intergrowth

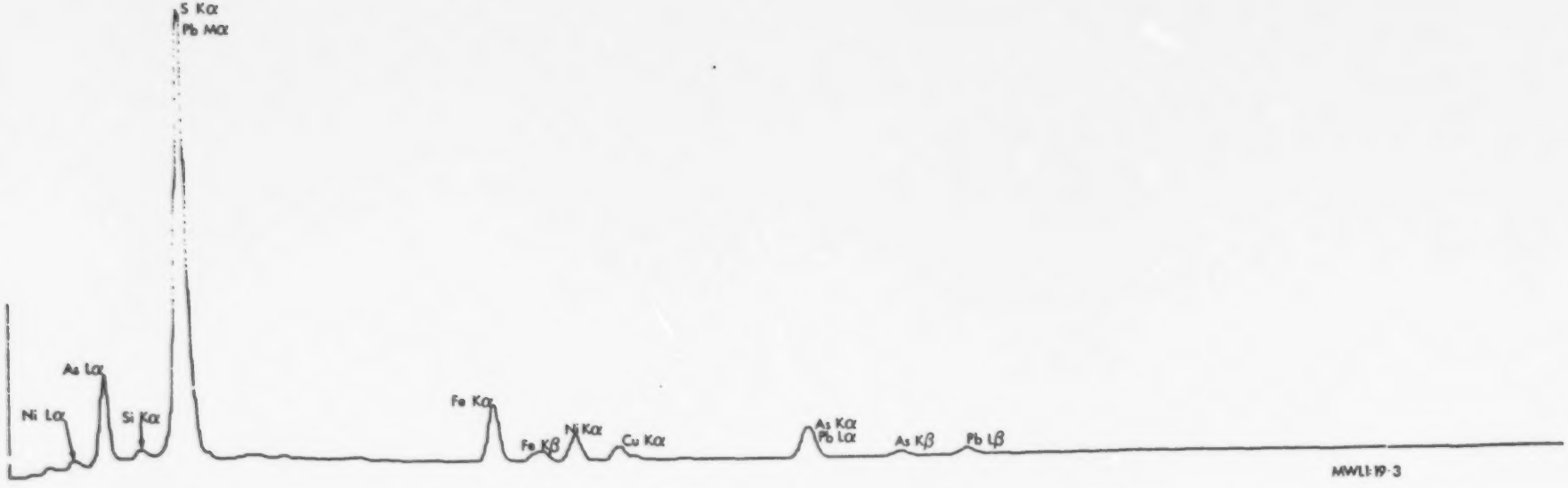

v. f. s 65k

COFFINITE – GALENA – GERSDORFFITE intergrowth

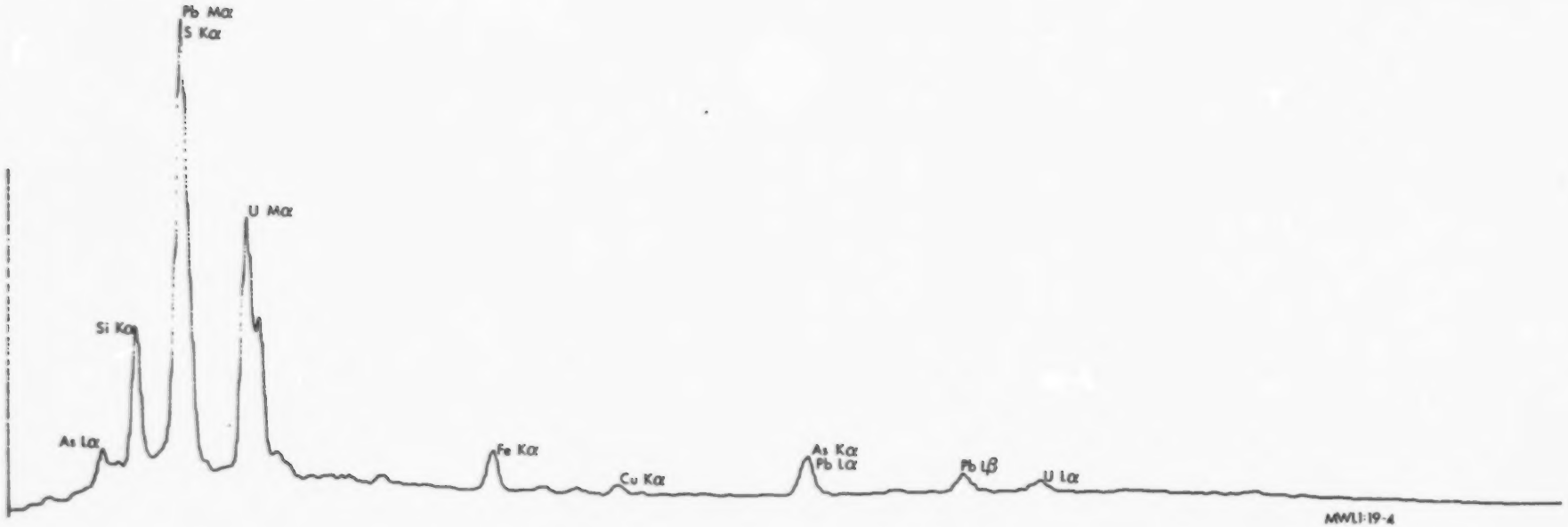

v. f. s. 32k

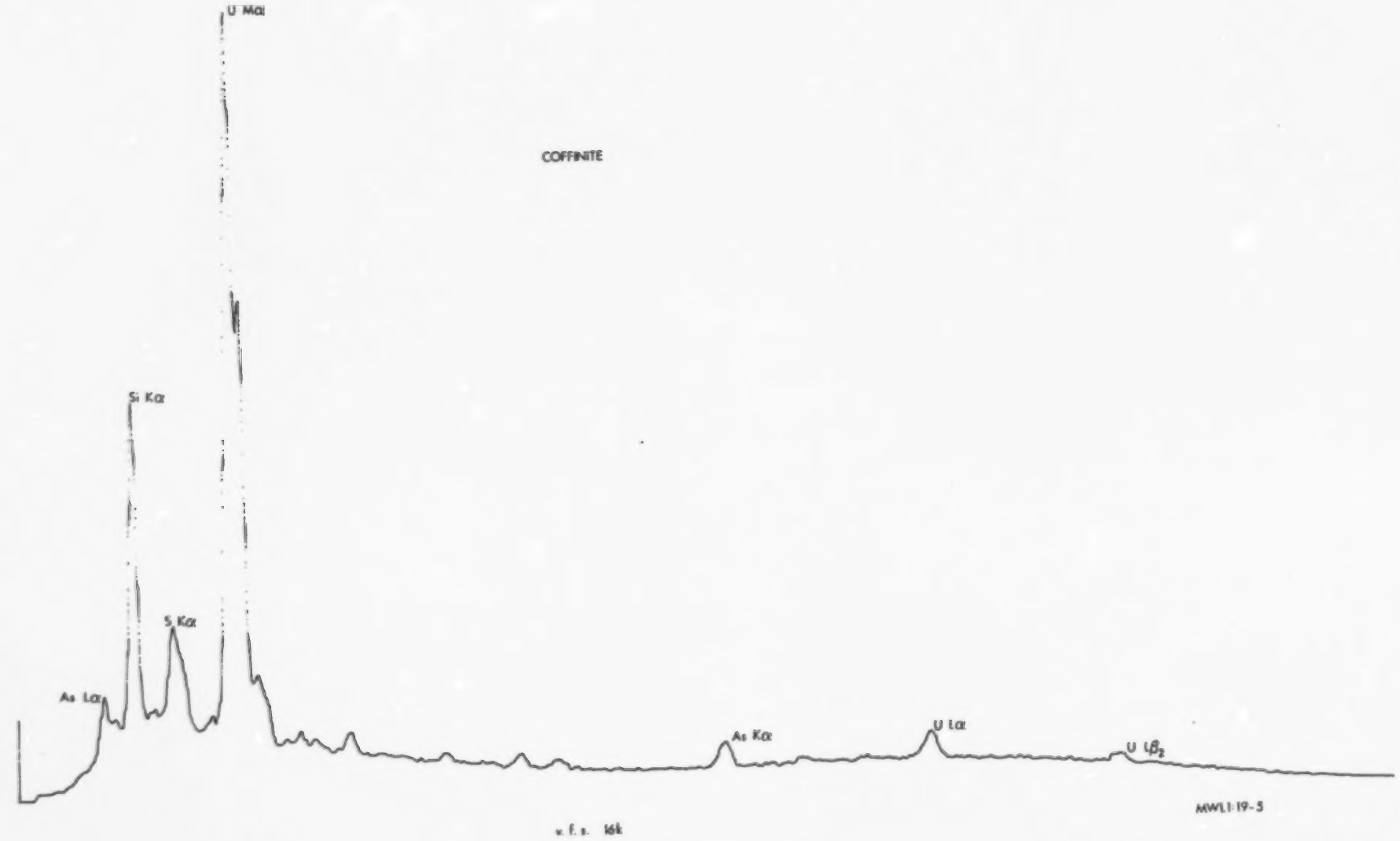
U Mα
COFFINITE
Si Kα
S Kα
As Lα
As Kα
U Lα
U Lβ2
MWL1-19-5
v. f. s. 16k

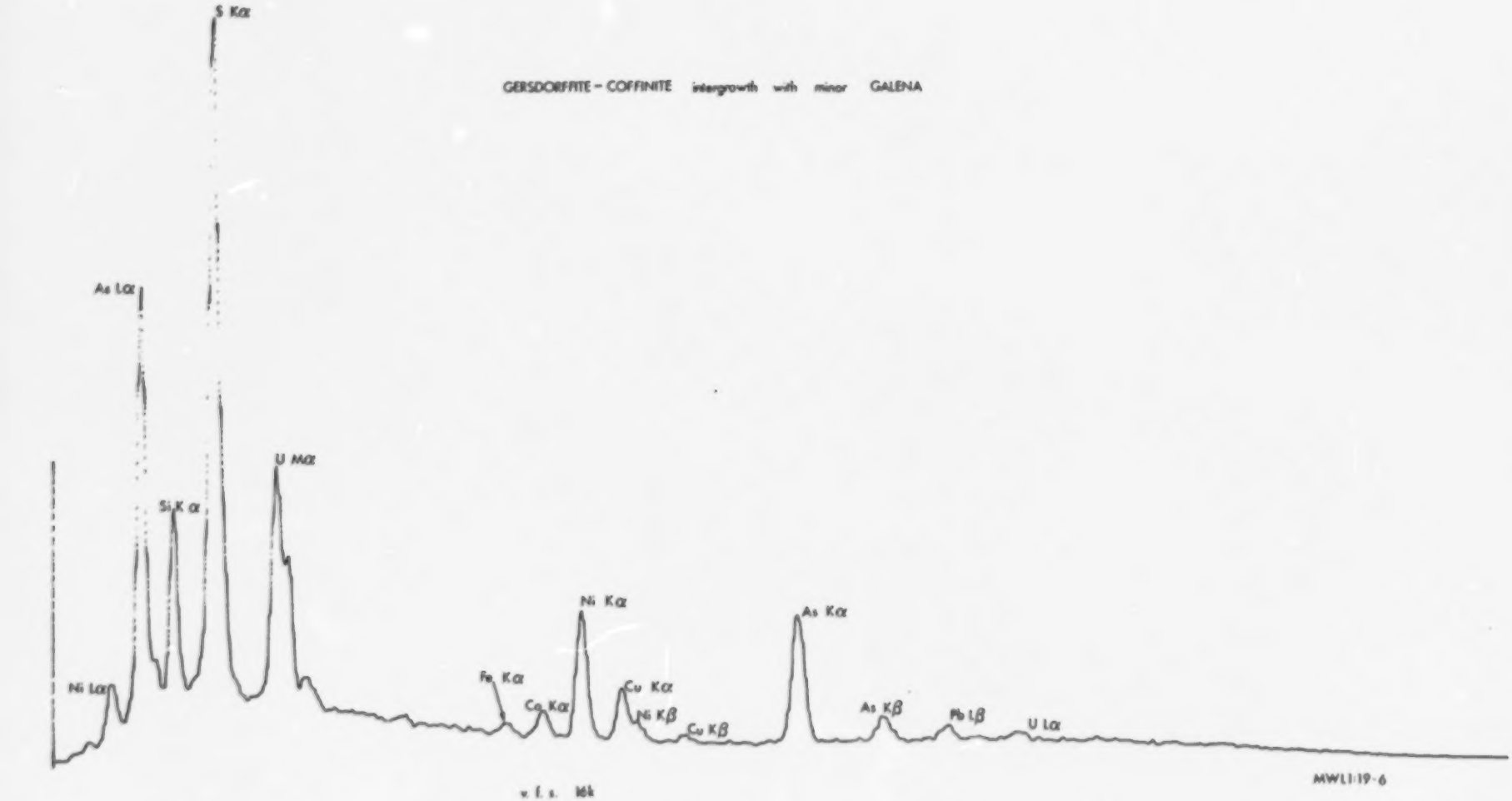
GERSDORFFITE – COFFINITE intergrowth with minor GALENA
S Kα
As Lα
U Mα
Si Kα
Ni Lα
Fe Kα
Co Kα
Ni Kα
Cu Kα
Ni Kβ
Cu Kβ
As Kα
As Kβ
Pb Lβ
U Lα
v. f. s. 16k
MWL1:19-6

PITCHBLENDE – COFFINITE intergrowth

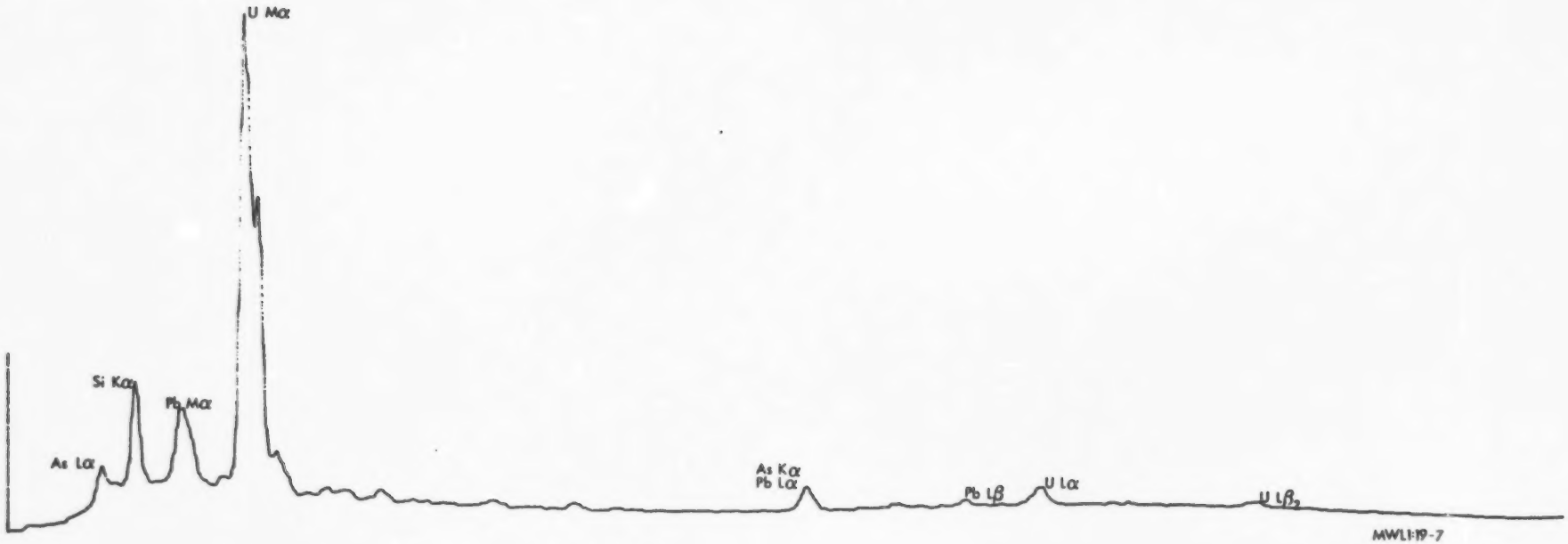

v. f. s. 32k

GERSDORFFITE with minor COFFINITE and GALENA

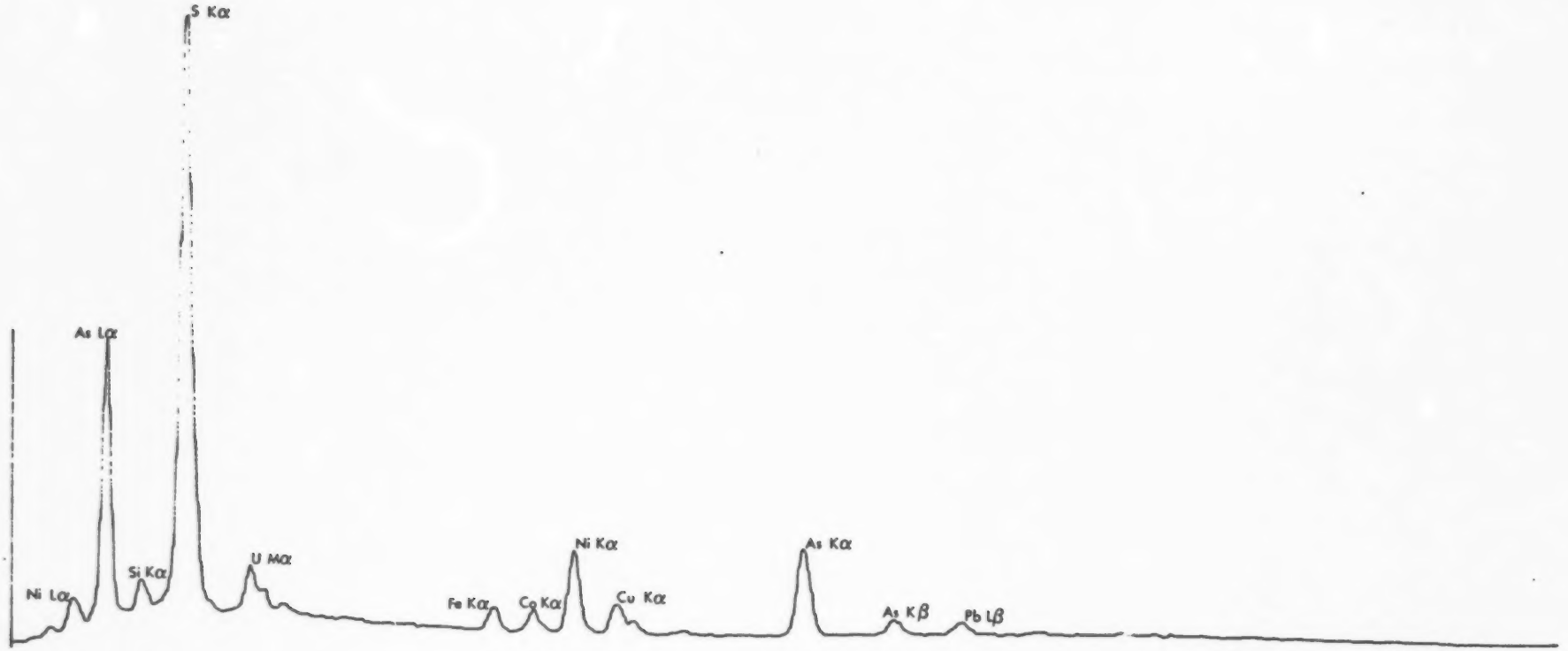

v. f. s. 32k

GERSDORFFITE

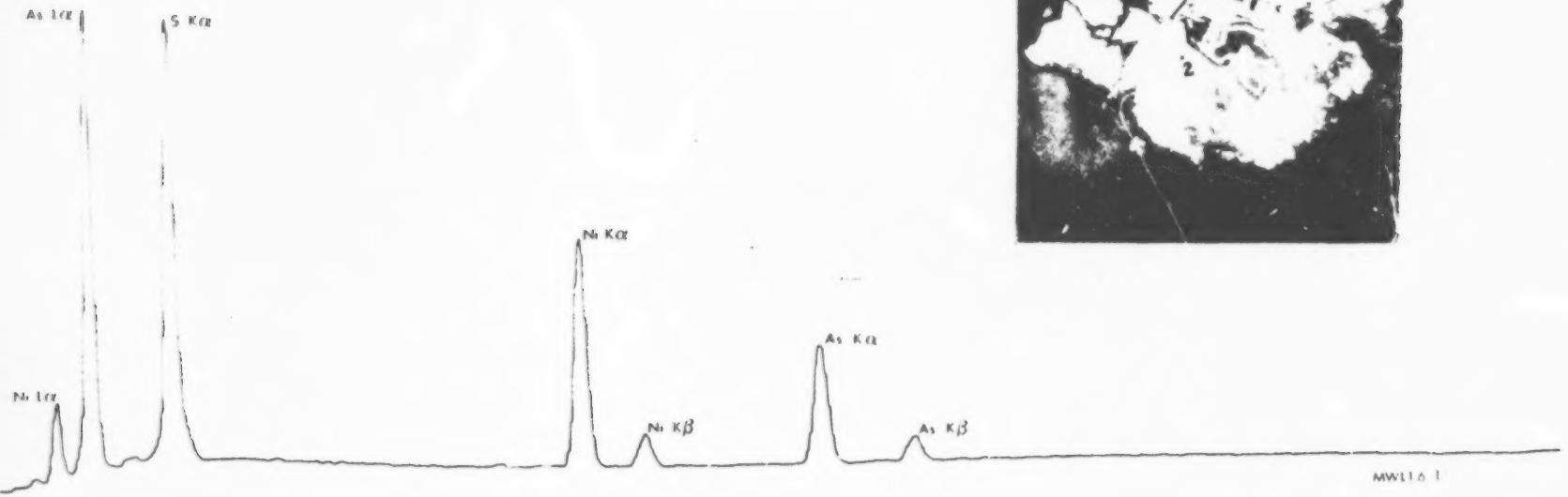

v I s 324

GERSDORFFITE

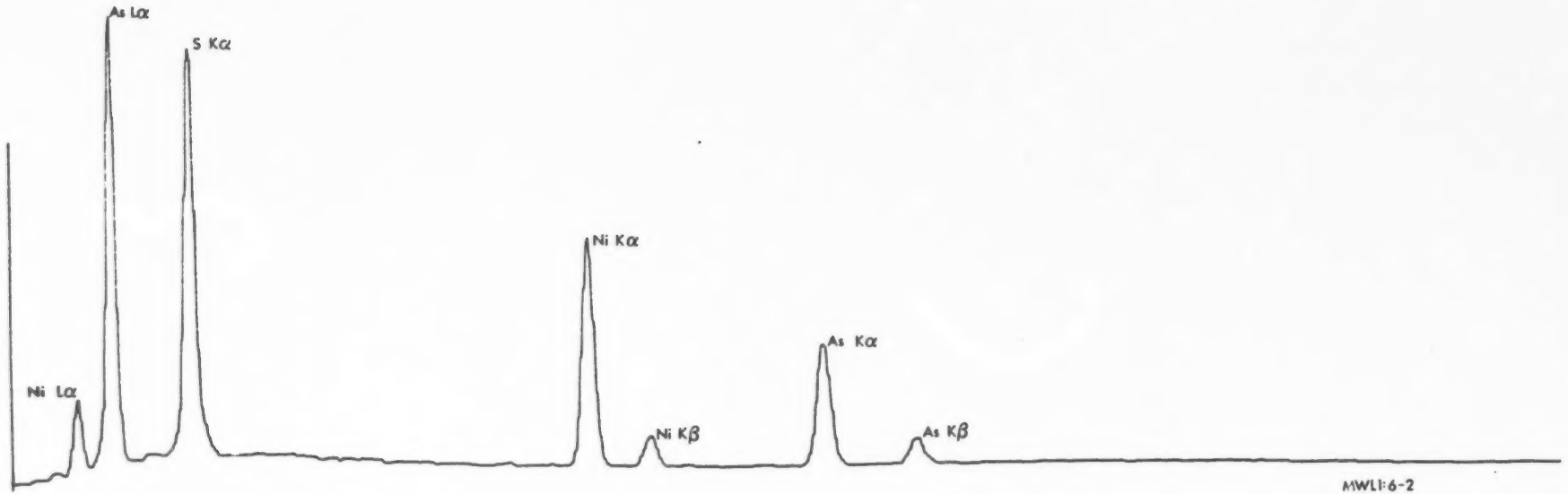

v. f. s. 32k

POOR
QUALITY
ORIGINAL